Chapter One

1.1. Introduction

The coronary artery disease is the most common type of the heart problem causing death in both sexes male or female of Sudanese people. This disease is mainly resulting when the artery that carry the blood supply to heart muscle become hardened, narrowed and weekend. This is mainly due to buildup of cholesterol and other material called plaque on their inner walls and this lead to condition called atherosclerosis, as this condition is developed leading to reduction of blood flow throw the artery resulting in reduction of blood supply and oxygenation to cardiac muscles which can lead to chest pain, angina and cardiac attack. The coronary heart disease also can lead to weaken the heart muscles and this will contributed in heart failure and arrhythmia.

As historical background Sir Godfrey Hounsfield is credited with the invention of the CT scanner in late 1960s. Since CT uses X-ray absorption to create images, the differences in the image brightness at any point will depend on physical density and the presence of atoms with a high difference in anatomic number like calcium, and soft tissue and water. The absorption of the X-ray beam by different atoms will cause differences in CT brightness on the resulting image (contrast resolution).

Blood and soft tissue (in the absence of vascular contrast enhancement) have similar density and consist of similar proportions of the same atoms (hydrogen, oxygen, carbon). Bone has an abundance of calcium and is thus brighter on CT. Fat has an abundance of hydrogen. Lung contains air, which is of extremely low physical density and appears black on CT (HU -1,000). The higher the density, the brighter the structure on CT. Calcium is bright white, air is black, and muscle or blood is gray. There are over 5,000 shades of this gray scale represented on CT, centered on zero (water). CT, therefore, can distinguish blood from air, fat, and bone, but not

readily from muscle or other soft tissue. The densities of blood, myocardium, thrombus, and fibrous tissues are so similar in their CT number that non-enhanced CT cannot distinguish these structures. Thus, the ventricles and other cardiac chambers can be seen on non-enhanced CT, but delineating the wall from the blood pool is not possible. Investigators have validated the measurement of "LV size" with cardiac CT, which is the sum of both left ventricle (LV) mass and volume Mao S, et.al (2000). Due to the thin wall, which does not contribute significantly to the total measured volume, the left and right atrial volumes can be accurately measured on non-contrast CT, Budoff MJ et.al (1999).

The basic principle of CT is that a fan-shaped, thin X-ray beam passes through the body at many angles to allow for cross-sectional imaging. The corresponding X-ray transmission measurements are collected by a detector array. Information entering the detector array and X-ray beam itself is collimated to produce thin sections while avoiding unnecessary photon scatter (to keep radiation exposure and image noise to a minimum). The x-ray tube and detector array rotate around the patient separated by 180°, allowing continuous acquisition of data. The data recorded by the detectors are digitized into picture elements (pixels) with known dimensions. The gray-scale information contained in each individual pixel is reconstructed according to the attenuation of the X-ray tube along its path using a standardized technique termed "filtered back projection." Grayscale values for pixels within the reconstructed tomogram are defined with reference to the value for water and are called "Hounsfield units" (HU; for the 1979 Nobel Prize winner, Sir Godfrey N. Hounsfield), or simply "CT numbers." These CT numbers are the attenuation or brightness of the individual pixel (smallest definable unit on CT) of data. A 3D pixel is called a voxel. Typical pixel values for studies commonly seen on cardiac CT. Because contrast resolution uses attenuation or density to visualize structures in gray scale, limitations of contrast resolution exist even on contrast enhanced studies.

These include differentiating the cardiac vessels from cardiac cavities with same density (such as when the arteries run become intra-myocardial) and differentiating non-calcified plaque from surrounding low density structures, including thrombus. Even with good contrast enhancement, differentiating different types of plaque (lipid-laden and fibrous) can sometimes be challenging, although it is always easy to differentiate the bright white plaques (calcified) from non-calcific plaques. The higher spatial resolution of CT allows visualization of coronary arteries both with and without contrast enhancement. The ability to see the coronary arteries on a non-contrast study depends upon the fat surrounding the artery (of lower density, thus more black on images), providing a natural contrast between the myocardium and the epicardial artery. Usually, the entire course of each coronary artery is visible on non-enhanced scans. The major exception is bridging, when the coronary artery delves into the myocardium and cannot be distinguished without contrast. The distinction of blood and soft tissue (such as the left ventricle, where there is no air or fat to act as a natural contrast agent) requires injection of contrast with CT. Similarly, distinguishing the lumen and wall of the coronary artery also requires contrast enhancement. The accentuated absorption of X-rays by elements of high atomic number like calcium and iodine allows excellent visualization of small amounts of coronary calcium as well as the contrast-enhanced lumen of medium-size coronary arteries. Air attenuates the X-ray less than water, and bone attenuates it more than water, so that in a given patient, Hounsfield units may range from −1,000 HU (air) through 0 HU (water) to above +1,000 HU (bone cortex). Coronary artery calcium in coronary atherosclerosis (consisting of the same calcium phosphate as in bone) has CT number >130 HU, typically going as high as +1,000 HU. It does not go as high as the bony cortex of the spine due to the smaller quantity and mostly inhomogeneous distribution in the coronary artery plaque. Metal, such as that found

in valves, wires, stents, and surgical clips, typically have densities of +1,000 HU or higher. Budoff MJ et.al (1999).

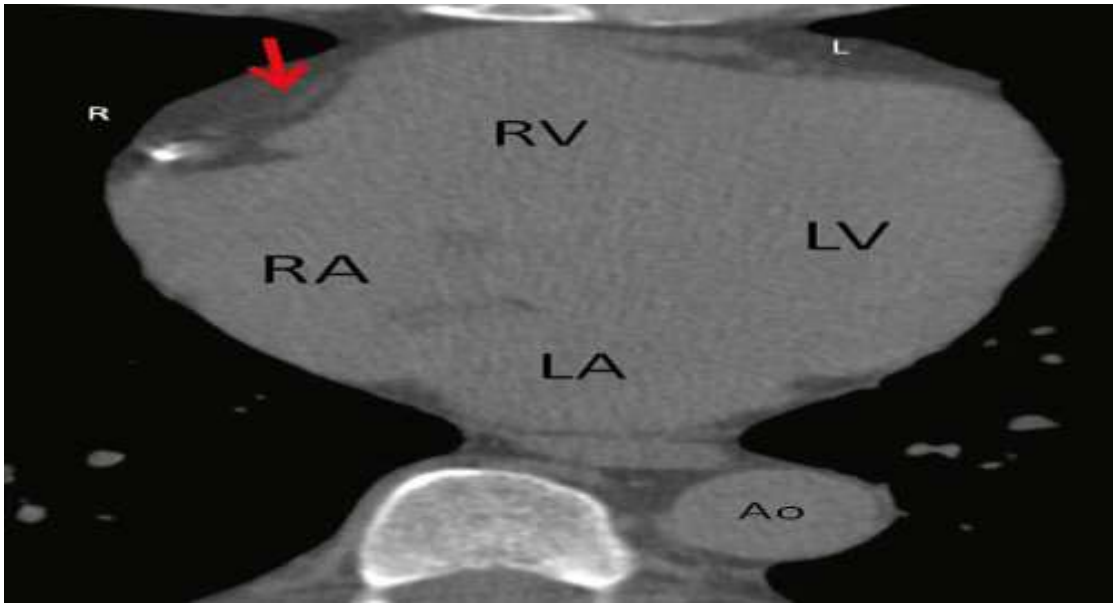

Figure 1.1. A non-contrast CT scan of the heart.

Quite a bit of information can be garnered without contrast. The pericardium is visible as a thin line (red arrow). The coronary arteries can be seen, and diameters and calcifications are present (R). The right coronary artery is seen near the R, and the left anterior at the L. The four chambers of the heart are also seen, and relative sizes can be measured from this non-contrast study. The descending aorta is also present on this image and can be evaluated and measured. Higher levels would allow visualization of the ascending aorta, pulmonary artery and superior vena cava on the same study. Ao aorta, L left anterior descending artery, LA left atrium, LV left ventricle, RA right atrium, and RV right ventricle. (Budoff et.al (1999)).

This study will evaluate the Role MDCT scanner which in fact has features such as faster image acquisition; physiological image and ability of characterize the lesion using CT number and calcium score which will use in the study based on patient data (age, gender and patient underlying disease) corresponded to CAD.

1.2. Problem of study:

The coronary artery disease is consider critical medical situation require precision and rapidity whatever the modalities use for diagnosis. The multi-detector computed tomography offer numerous value by measuring calcium score, diameter of arteries and degree of stenosis by using advanced modalities such as (MIP, MPR and VR). Severe calcifications and higher heart rates are known to degrade image quality and limit correct diagnosis in conventional angiography as a result the conventional angiography is more invasive in procedure and not safety for staff and patient, if the patients are selected carefully the overall ability of coronary segment visualization as well as lesion detection could be performed. Therefore MDCT scanner have another advantages of faster and accurate acquisition which make it is so importance to evaluate this degree of precision and quickness base on features of device over other.

1.3. Objectives of the Study:

1.3.1. General objective:

The main aims of this study was to characterize the role of multi-detector CT scan in diagnosing of coronary artery disease in Sudanese population in order to classify the plaque type and to characterize the disease according to is calcium score.

1.3.2. Specific Objectives:

- To study the common diseases in coronary artery in Sudanese population
- To estimate the most affected arteries and to evaluate the type & localization of lesions (plaque).
- To characterize the lesion by measuring of calcium score related to each patient history and CT findings.

- To find correlation between patient age, gender and CAD.
- To correlate between plague type with degree of stenosis
- To characterize lesion by using (MPR) Multiplaner reconstruction, (MIP) maximum intensity projection, and (VR) Volume rendered facilities.

1.4. Significant of study:

This study was highlighted on evaluation of coronary artery disease using MDCT scanner, once we need faster and accurate diagnostic modalities in this situation in order to have high diagnostic accuracy in assessing coronary artery disease since MDCT has been proposed as an alternative to conventional coronary angiography (CA) for the diagnosis of CAD.

1.5. Overview of the study:

This study was consist of five chapters, chapter one was an introduction introduce briefly this thesis and contained (anatomy, physiology, pathology problem of study also contain general, specific objectives, significant of the study and overview of the study). Chapter two was literature review about role of MDCT scanner in diagnosis of CAD, and other modalities used. Chapter three was describe the methodology (material, method) used in this study. Chapter four was included result of presentation of final finding of study; chapter five included discussion, conclusion and recommendation for future scope in addition to references and appendices.

Chapter Two

2.1. Anatomy

The heart is a muscular pump that ejects blood into the vascular tree with sufficient pressure to maintain optimal circulation. Average weight of the heart in an adult male is 300-350 gm while that of an adult female is 250-300 gm. Heart is divided into four chambers: a right and a left atrium both lying superiorly, and a right and a left ventricle both lying inferiorly and are larger. The atria are separated by a thin interatrial partition called interatrial septum, while the ventricles are separated by thick muscular partition called interventricular septum. The thickness of the right ventricular wall is 0.3 to 0.5 cm while that of the left ventricular wall is 1.3 to 1.5 cm. The blood in the heart chambers moves in a carefully prescribed pathway:

venous blood from systemic circulation → right atrium → right ventricle → pulmonary arteries → lungs → pulmonary veins → left atrium → left ventricle → aorta → systemic arterial supply. Wall of the heart consists mainly of the myocardium which is covered externally by thin membrane, the epicardium or visceral pericardium, and lined internally by another thin layer, the endocardium.

The transport of blood is regulated by cardiac valves: two loose flap-like atrioventricular valves, tricuspid on the right and mitral (bicuspid) on the left; and two semilunar valves with three leaflets each, the pulmonary and aortic valves, guarding the outflow tracts. The normal circumference of the valvular openings measures about 12 cm in tricuspid, 8.5 cm in pulmonary, 10 cm in mitral and 7.5 cm in aortic valve.

The myocardium is the muscle tissue of the heart composed of syncytium of branching and anastomosing, transversely striated muscle fibres arranged in parallel fashion. The space between myocardial fibres contains a rich capillary network and loose connective tissue. The myocardial fibres are connected to each other by

irregular joints called as intercalated discs. They represent apposed cell membranes of individual cells which act as tight junctions for free transport of ions and action potentials. The cardiac myocyte is very rich in mitochondria which is the source of large amount of ATP required for cardiac contraction. The cardiac muscle fibre has abundant sarcoplasmic reticulum corresponding to endoplasmic reticulum of other cells. Transverse lines divide each fibre into sarcomeres which act as structural and functional subunits. Each sarcomere consists of prominent central dark A-band attributed to thick myosin filaments and flanked on either side by light I-bands consisting of thin actin filament. The actin bands are in the form of twisted rods overlying protein molecules called tropomyosin. These protein molecules are of 3 types: troponin-I, troponin- T, and troponin-C. Troponin molecules respond to calcium ions in cyclical contraction-relaxation of myocardial fibres. Myocardial fibres are terminally differentiated cells and do not regenerate but there is recent evidence that new cardiac myocytes can be formed from stem cells recruited from the circulation. The conduction system of the heart located in the myocardium is responsible for regulating rate and rhythm of the heart. It is composed of specialized Purkinje fibres which contain some contractile myofilaments and conduct action potentials rapidly. The conduction system consists of 4 major components: ((Stuon et.al (1990), fouad et.al (2000)).

The sinoatrial (SA) node is located in the posterior wall of the right atrium adjacent to the point at which the superior vena cava enters the heart. It is also called cardiac pacemaker since it is responsible for determining the rate of contraction for all cardiac muscle. The atrioventricular (AV) bundle conducts the impulse from the SA node to the AV node, the atrioventricular (AV) node is located on the top of the interventricular septum and receives impulses from the SA node via AV bundle and transmits them to the bundle of His and the bundle of His extends through the interventricular septum and divides into right and left bundle branches which

arborise in the respective ventricular walls. These fibres transmit impulses from the AV node to the ventricular walls.

The pericardium consists of a closely apposed layer, visceral pericardium or epicardium, and an outer fibrous sac, the parietal pericardium. The two layers enclose a narrow pericardial cavity which is lined by mesothelial cells and normally contains 10-30 ml of clear, watery serous fluid. This fluid functions as lubricant and shock absorbant to the heart. The endocardium is the smooth shiny inner lining of the myocardium that covers all the cardiac chambers, the cardiac valves, the chordae tendineae and the papillary muscles. It is lined by endothelium with connective tissue and elastic fibres in its deeper part. The valve cusps and semilunar leaflets are delicate and translucent structures. The valves are strengthened by collagen and elastic tissue and covered by a layer of endothelium (valvular endocardium).

2.1.1. Myocardial blood supply:

The cardiac muscle, in order to function properly, must receive adequate supply of oxygen and nutrients. Blood is transported to myocardial cells by the coronary arteries which originate immediately above the aortic semilunar valve. Most of blood flow to the myocardium occurs during diastole.

The major coronary trunks, which supplying blood to specific segments of the heart: The anterior descending branch of the left coronary artery supplies most of the apex of the heart, the anterior surface of the left ventricle, the adjacent third of the anterior wall of the right ventricle, and the anterior two-third of the interventricular septum. The circumflex branch of the left coronary artery supplies the left atrium and a small portion of the lateral aspect of the left ventricle). The right coronary artery supplies the right atrium, the remainder of the anterior surface of the right ventricle, the adjacent half of the posterior wall of the left ventricle and the posterior third of the interventricular septum. There are 3 anatomic patterns of distribution of the coronary blood supply, depending upon which of the coronary arteries crosses the crux. Crux

is the region on the posterior surface of the heart where all the four cardiac chambers and the interatrial and interventricular septa meet. These patterns are as under:

Right coronary artery preponderance is the most common pattern. In this, right coronary artery supplies blood to the whole of right ventricle, the posterior half of the interventricular septum and a part of the posterior wall of the left ventricle by crossing the crux, balanced cardiac circulation is the next most frequent pattern. In this, the right and left ventricles receive blood supply entirely from right and left coronary arteries respectively. The posterior part of the interventricular septum is supplied by a branch of the right coronary while the anterior part is supplied by a branch of the left coronary artery, Left coronary preponderance is the least frequent pattern. In this, the left coronary artery supplies blood to the entire left ventricle, whole of interventricular septum and also supplies blood to a part of the posterior wall of the right ventricle by crossing the crux. Coronary veins run parallel to the major coronary arteries to collect blood after the cellular needs of the heart are met. Subsequently, these veins drain into the coronary sinus.

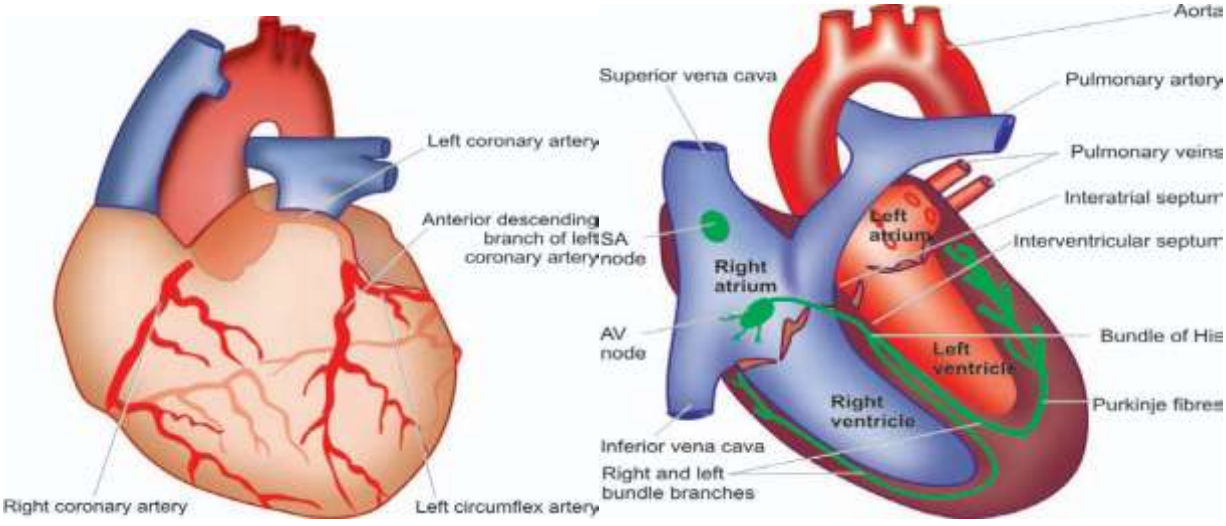

Figure 2.1. Show the heart blood vessels and general anatomy (L. Drake et.al 2014)

2.2. Pathology of the heart:

For the purpose of pathologic discussion of heart diseases, they are categorized on the basis of anatomic region involved and the functional impairment. Accordingly, topics on heart diseases are discussed in this chapter under the following headings: Heart failure, Congenital heart diseases, Ischemic heart disease, Hypertensive heart disease, Corpulmonale, Rheumatic fever and rheumatic heart disease, Non-rheumatic endocarditis, Valvular diseases and deformities, Myocardial disease, Pericardial disease, Tumours of the heart and Pathology of cardiovascular interventions. It may be mentioned here that pattern of heart diseases in developing and developed countries is distinct due to difference in living standards. In children, valvular diseases are common all over the world, but in developing countries including India, infections, particularly rheumatic valvular disease, is the dominant cause compared to congenital etiology in affluent countries. On the other hand, ischemic heart disease and hypertensive cardiomyopathy are the major heart diseases in adults in western populations. Chopra P et.al (2003)

2.2.1. Heart failure:

Heart failure is defined as the pathophysiologic state in which impaired cardiac function is unable to maintain an adequate circulation for the metabolic needs of the tissues of the body. It may be acute or chronic. The term congestive heart failure (CHF) is used for the chronic form of heart failure in which the patient has evidence of congestion of peripheral circulation and of lungs. CHF is the end-result of various forms of serious heart diseases.

2.2.1.1. Etiology:

Heart failure may be caused by one of the following factors, either singly or in combination: Intrinsic pump failure; the most common and most important cause of heart failure is weakening of the ventricular muscle due to disease so that the heart

fails to act as an efficient pump. The various diseases which may culminate in pump failure by this mechanisms are as under: Ischemic heart disease, Myocarditis, Cardiomyopathies, Metabolic disorders e.g. beriberi and Disorders of the rhythm e.g. atrial fibrillation and flutter. Increased workload on the heart: Increased mechanical load on the heart results in increased myocardial demand resulting in myocardial failure. Increased load on the heart may be in the form of pressure load or volume load. Increased pressure load may occur in the following states: Systemic and pulmonary arterial hypertension, Valvular disease e.g. mitral stenosis, aortic stenosis, pulmonary stenosis and chronic lung diseases.

Increased volume load occurs when a ventricle is required to eject more than normal volume of the blood resulting in cardiac failure. This is seen in the following conditions: Valvular insufficiency, severe anemia, Thyrotoxicosis, Arteriovenous shunts, Hypoxia due to lung diseases. Impaired filling of cardiac chambers: Decreased cardiac output and cardiac failure may result from extra-cardiac causes or defect in filling of the heart: Cardiac tamponade e.g. haemopericardium, hydropericardium and Constrictive pericarditis.

2.2.1.2. Types of Heart Failure:

Heart failure may be acute or chronic, right-sided or left sided, and forward or backward failure. Depending upon whether the heart failure develops rapidly or slowly, it may be acute or chronic: Acute heart failure. Sudden and rapid development of heart failure occurs in the following conditions: Larger myocardial infarction, Valve rupture, Cardiac tamponade, Massive pulmonary embolism, acute viral myocarditis and acute bacterial toxemia.

In acute heart failure, there is sudden reduction in cardiac output resulting in systemic hypotension but oedema does not occur. Instead, a state of cardiogenic shock and cerebral hypoxia develops.

Chronic heart failure. More often, heart failure develops slowly as observed in the following states: Myocardial ischemia from atherosclerotic coronary artery disease, Multi-valvular heart disease, and Systemic arterial hypertension, chronic lung diseases resulting in hypoxia and pulmonary arterial hypertension and Progression of acute into chronic failure. In chronic heart failure, compensatory mechanisms like tachycardia, cardiac dilatation and cardiac hypertrophy try to make adjustments so as to maintain adequate cardiac output. This often results in well-maintained arterial pressure and there is accumulation of oedema.

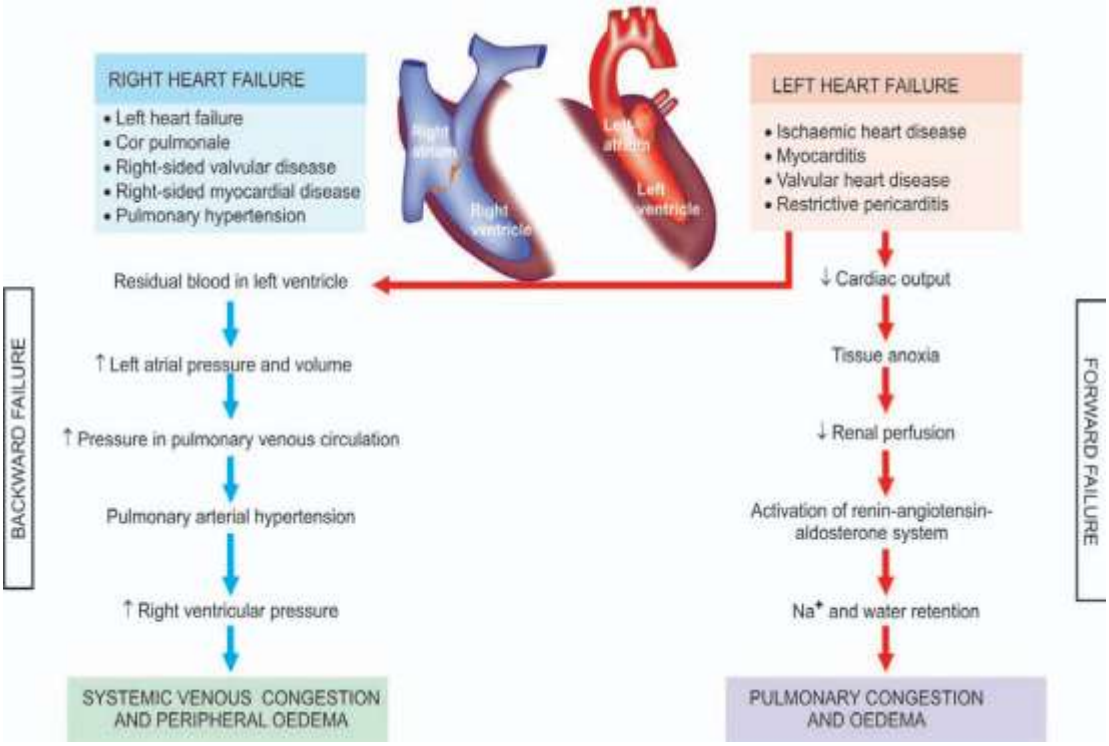

Figure 2.2. Show the type and mechanism of heart failure

2.2.2. Congenital Heart Disease:

Congenital heart disease is the abnormality of the heart present from birth. It is the most common and important form of heart disease in the early years of life and is present in about 0.5% of newborn children. The incidence is higher in premature infants. The cause of congenital heart disease is unknown in majority of cases. It is

attributed to multifactorial inheritance involving genetic and environmental influences. Other factors like rubella infection to the mother during pregnancy, drugs taken by the mother and heavy alcohol drinking by the mother, have all been implicated in causing in utero fetal injury resulting in congenital malformations of the heart. And the congenital heart disease may classified as: Congenital anomalies of the heart may be either shunts (left-to-right or right-to-left), or defects causing obstructions to flow. However, complex anomalies involving combinations of shunts and obstructions are also often present. A simple classification of important and common examples of these groups is given below: Mal-positions of the heart, shunts (cyanotic congenital heart disease). Left-to-right shunts (Acyanotic or late cyanotic group): Ventricular septal defect (VSD) (25-30%), atrial septal defect (ASD) (10-15%) and Patent ductus arteriosus (PDA) (10-20%). Right-to-left shunts (Cyanotic group), Tetralogy of Fallot (6-15%), Transposition of great arteries (4-10%), Persistent truncus arteriosus (2%), Tricuspid atresia and stenosis (1%). Obstructions (obstructive congenital heart disease): Coarctation of aorta (5-7%), Aortic stenosis and atresia (4-6%), pulmonary stenosis and atresia (5-7%)

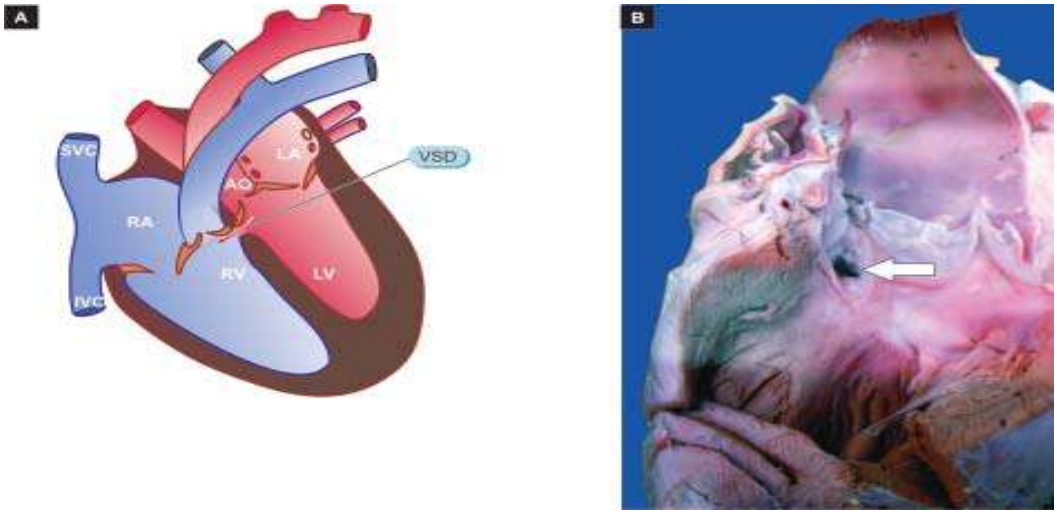

Figure 2.3. Ventricular septal defect. A, Schematic representation (LA = Left atrium; LV = Left ventricle; AO = Aorta; PV = Pulmonary valve; PT = Pulmonary trunk;

RA = Right atrium; RV = Right ventricle; SVC = Superior vena cava; IVC = Inferior vena cava). B, The opened up chambers of the heart show a communication in the inter-ventricular septum superiorly (see arrow).

2.2.3. Ischemic Heart Disease (IHD):

Ischemic heart disease IHD is defined as acute or chronic form of cardiac disability arising from imbalance between the myocardial supply and demand for oxygenated blood. Since narrowing or obstruction of the coronary arterial system is the most common cause of myocardial anoxia, the alternate term 'coronary artery disease CAD' is used synonymously with IHD. IHD or CAD is the leading cause of death in most developed countries (about one-third of all deaths) and somewhat low incidence is observed in the developing countries. Men develop IHD earlier than women and death rates are also slightly higher for men than for women until the menopause. As per rising trends of IHD worldwide, it is estimated that by the year 2020 it would become the most common cause of death throughout world. (Corri et.al (2003)).

2.2.3.1. Etiopathogenesis:

IHD is invariably caused by disease affecting the coronary arteries, the most prevalent being atherosclerosis accounting for more than 90% cases, while other causes are responsible for less than 10% cases of IHD. Therefore, it is convenient to consider the etiology of IHD under three broad headings: Coronary atherosclerosis; Superadded changes in coronary atherosclerosis; and Non-atherosclerotic causes.

2.2.3.1.1. Coronary Atherosclerosis:

Coronary atherosclerosis resulting in 'fixed' obstruction is the major cause of IHD in more than 90% cases. The general aspects of atherosclerosis as regards its etiology, pathogenesis and the morphologic features of atherosclerotic lesions have already been dealt with at length this study. Here, a brief account of the specific

features in pathology of lesions in atherosclerotic coronary artery disease in particular are presented. Its distribution: Atherosclerotic lesions in coronary arteries are distributed in one or more of the three major coronary arterial trunks, the highest incidence being in the anterior descending branch of the left coronary, followed in decreasing frequency, by the right coronary artery and still less in circumflex branch of the left coronary. About one third of cases have single-vessel disease, most often left anterior descending arterial involvement; another one-third have two vessel disease, and the remainder have three major vessel disease. Location: Almost all adults show atherosclerotic plaques scattered throughout the coronary arterial system. However, significant stenotic lesions that may produce chronic myocardial ischemia show more than 75% (three-fourth) reduction in the cross-sectional area of a coronary artery or its branch. The area of severest involvement is about 3 to 4 cm from the coronary ostia, more often at or near the bifurcation of the arteries, suggesting the role of hemodynamic forces in atherogenesis. Fixed atherosclerotic plaques: The atherosclerotic plaques in the coronaries are more often eccentrically located bulging into the lumen from one side. Occasionally there may be concentric thickening of the wall of the artery. Atherosclerosis produces gradual luminal narrowing that may eventually lead to 'fixed' coronary obstruction. The general features of atheroma's of coronary arteries are similar to those affecting elsewhere in the body and may develop similar complications like calcification, coronary thrombosis, ulceration, hemorrhage, rupture and aneurysm formation. (Corri et.al (2003))

2.2.3.1.2. Superadded Changes in Coronary Atherosclerosis:

The attacks of acute coronary syndromes, which include acute myocardial infarction, unstable angina and sudden ischaemic death, are precipitated by certain changes superimposed on a pre-existing fixed coronary atheromatous plaque. These changes are as under: Acute changes in chronic atheromatous plaque. Though chronic fixed

obstructions are the most frequent cause of IHD, acute coronary episodes are often precipitated by sudden changes in chronic plaques such as plaque Haemorrhage, fissuring, or ulceration that results in thrombosis and embolization of athermanous debris. Acute plaque changes are brought about by factors such as sudden coronary artery spasm, tachycardia, intraplaque Haemorrhage and hypercholesterolemia, Coronary artery thrombosis. Transmural acute myocardial infarction is often precipitated by partial or complete coronary thrombosis. The initiation of thrombus occurs due to surface ulceration of fixed chronic athermanous plaque, ultimately causing complete luminal occlusion. The lipid core of plaque, in particular, is highly chromogenic. Small fragments of thrombotic material are then dislodged which are embolized to terminal coronary branches and cause micro infarcts of the myocardium. Corri et.al (2003)

Table 1.1. American Heart Association Classification (1995) of Human Atherosclerosis, jonhn et.al (1996)

Type	**Main Histology**	**Main pathogenesis**	**Age at onset**	**clinical**
Type I: initial lesions	Macrophages, occasional, toam cell	Accumulation of lipoprotein	1st decade	Asymptomatic
Type II: fatty streaks	Many layers of macrophages and foam cells	Accumulation of lipoprotein	1st decade	Asymptomatic
Type III: intermediate lesions	Many lipid-laden cells and scattered extracellular lipid droplets	Accumulation of lipoprotein	2st decade	Asymptomatic
Type IV: athermanous lesions	Intra-as well as extracellular lipid pool	Accumulation of lipid	2st decade	Asymptomatic, or manifest symptoms

Type V: fibrofatty lesions	Fibrotic cap and lipid core (V a), may have calcification (V b)	Smooth muscle cell proliferation and increased collagen	3st decade	Asymptomatic, or manifest symptoms
Type VI: complicated lesions	Ulceration, hemorrhage, hematoma, thrombosis	Hemorrhage, stress, thrombosis, hematoma	3st decade	Asymptomatic, or manifest symptoms

Local platelet aggregation and coronary artery spasm: Some cases of acute coronary episodes are caused by local aggregates of platelets on the atheromatous plaque, short of forming a thrombus. The aggregated platelets release vasospasmic mediators such as thromboxane A2 which may probably be responsible for coronary vasospasm in the already atherosclerotic vessel. Based on progressive pathological changes and clinical correlation, American Heart Association (1995) has classified human coronary atherosclerosis into 6 sequential types in ascending order of grades of lesions. American Heart Association (1995)

2.2.3.1.2. Non-atherosclerotic Causes:

Several other coronary lesions may cause IHD in less than 10% of cases. These are as under: Vasospasm. It has been possible to document vasospasm of one of the major coronary arterial trunks in patients with no significant atherosclerotic coronary narrowing which may cause angina or myocardial infarction, Stenosis of coronary ostia. Coronary ostial narrowing may result from extension of syphilitic aortitis or from aortic atherosclerotic plaques encroaching on the opening, Arteritis. Various types of inflammatory involvements of coronary arteries or small branches like in rheumatic arteritis, polyarteritisnodosa, thrombo-angiitis obliterans (Buerger's disease), Takayasu's disease, Kawasaki's disease, tuberculosis and other bacterial infections may contribute to myocardial damage, Embolism. Rarely, emboli originating from elsewhere in the body may occlude the left coronary artery and its branches and produce IHD. The emboli may originate from bland thrombi, or from

vegetations of bacterial endocarditis; rarely fat embolism and air embolism of coronary circulation, Thrombotic diseases. Another infrequent cause of coronary occlusion is from hypercoagulability of the blood such as in shock, polycythaemiavera, sickle cell anaemia and thrombotic thrombocytopenic purpura, Trauma: Contusion of a coronary artery from penetrating injuries may produce thrombotic occlusion, Aneurysms. Extension of dissecting aneurysm of the aorta into the coronary artery may produce thrombotic coronary occlusion. Rarely, congenital, mycotic and syphilitic aneurysms may occur in coronary arteries and produce similar occlusive effects and Compression. Compression of a coronary from outside by a primary or secondary tumour of the heart may result in coronary occlusion.

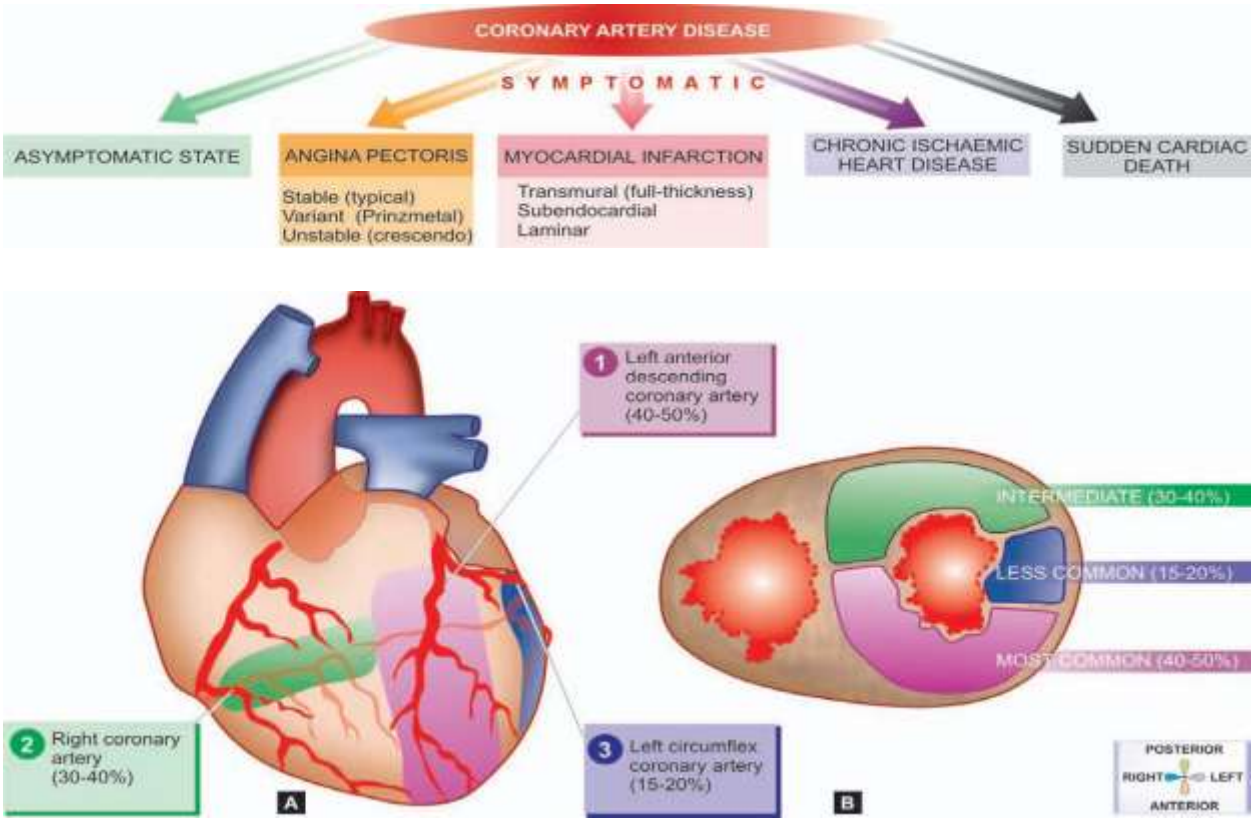

Figure 2.4. Common locations and the regions of involvement in myocardial infarction, the figure shows region of myocardium affected by stenosis of three

respective coronary trunks in descending order shown as: 1) left anterior descending coronary, 2) right coronary and 3) left circumflex coronary artery. A, as viewed from anterior surface. B, as viewed on transverse section at the apex of the heart.

2.2.4. Pathology of Cardiovascular Interventions:

Nowadays, with the development of surgical and nonsurgical coronary revascularization procedures in coronary artery disease, it has been possible to study the pathology of native as well as grafted vessel. However, these invasive therapeutic interventions are done in conjunction with life style changes for modifying the risk factors. Besides, the myocardial tissue by Endomyocardial biopsy is also accessible for histopathological study.

2.2.4.1. Endomyocardial biopsy:

Currently, it is possible to perform Endomyocardial biopsy (EMB) for making a final histopathological diagnosis in certain cardiac diseases. The main indications for EMB are: myocarditis, cardiac transplant cases, restrictive heart disease, infiltrative heart diseases such as in amyloidosis, storage disorders etc.

EMB is done by biopsy forceps introduced via cardiac catheter into either of the ventricles but preferably right ventricle is biopsied for its relative ease and safety. The route for the catheter may be through internal jugular vein or femoral vein for accessing the right ventricle.

2.2.4.2. Balloon angioplasty:

Balloon angioplasty or percutaneous coronary intervention (PCI) is a non-surgical procedure that employs percutaneous insertion and manipulation of a balloon catheter into the occluded coronary artery. The balloon is inflated to dilate the stenotic artery which causes endothelial damage, plaque fracture, medial dissection and hemorrhage in the affected arterial wall. PCI is accompanied with insertion of coronary stents in the blocked coronaries with a success rate of symptoms in over

95% cases. However, case selection for PCI is important and major indications are 2 or 3 vessel block but blockage of left main coronary is a contraindication for PCI. Unstable angioplasty may be associated with acute coronary syndromes. PCI is followed by administration of anti-platelet (oral aspirin) and antithrombin therapy to avoid occurrence of coronary thrombosis. Recurrent stenosis after metal stenting in PCI may occur within 6 months in about 20% patients, more often in patients of diabetes mellitus. Restenosis is multifactorial in etiology that includes smooth muscle cell proliferation, extracellular matrix and local thrombosis. However, widespread use of drug-delivering stents has made it possible to overcome several long-term complications of coronary stening. Currently, stents with anti-proliferative, anti-inflammatory, cytotoxic and cytostatic agents are commercially available.

2.2.4.3. Coronary Artery Bypass Grafting:

Coronary artery bypass grafting CABG employs the use of autologous grafts to replace or bypass the blocked coronary arteries. Most frequently used is autologous graft of saphenous vein which is reversed (due to valves in the vein) and transplanted, or left internal mammary artery may be used being in the operative area of the heart. Long-term follow-up of CABG surgery has yielded following observations on pathology of grafted vessel: In a reversed saphenous vein graft, long-term luminal patency is 50% after 10 years. Pathologic changes which develop in grafted vein include thrombosis in early stage, intimal thickening and graft atherosclerosis with or without complicated lesions, Internal mammary artery graft, however, has a patency of more than 90% after 10 years and Atherosclerosis with superimposed complications may develop in native coronary artery distal to the grafted vessel as well as in the grafted vessel.

2.2.4.4. Cardiac Transplantation:

Since the first human-to-human cardiac transplant was carried out successfully by South African surgeon Dr. Christian Barnard in 1967, cardiac transplantation and prolonged assisted circulation is being done in many countries in end-stage cardiac diseases, most often in idiopathic dilated cardiomyopathy, heart failure and IHD.

Worldwide, about 3,000 cardiac transplants are performed annually. The survival following heart transplants is reported as: 1 year in 85%, 5 years in 65% and 10 years in 45% cases. Major complications are transplant rejection reaction, infections (particularly with Toxoplasma gondii and cytomegaloviruses), graft coronary atherosclerosis and higher incidence of malignancy due to long-term administration of immunosuppressive therapy. One of the main problems in cardiac transplant centers is the availability of donors. The concept of cardiac stem cells resident in the heart and possibly of bone marrow stem cells transdifferentiating into cardiac myocyte has generated interest in treatment of patients of IHD with transplantation of these stem cells. Preliminary studies in IHD cases have yielded encouraging results in clinical improvement and reduction in infarct size and hold promise for future.

2.3. Cardiac CT:

Cardiac computed tomography CT provides image slices or tomograms of the heart. CT technology has significantly improved since its introduction into clinical practice in 1972. Current conventional scanners used for cardiac and cardiovascular imaging now employ either a rotating X-ray source with a circular, stationary detector array (spiral or helical CT) or a rotating electron beam EBCT. The attenuation map recorded by the detectors is then transformed through a filtered back-projection into the CT image used for diagnosis. The biggest issue with cardiac imaging is the need for both spatial and temporal resolution. Cardiac magnetic resonance MR has been an emerging technique for almost 2 decades, making little progress toward

widespread utilization over this time. Temporal resolution (how long it takes to obtain an image) is inversely related to spatial resolution with cardiac MR. Improving the MR spatial resolution requires prolonging the imaging time. This greatly limits the ability to focus with precision on moving objects, as the viewer needs to settle for either a high resolution image plagued by cardiac motion, or a low resolution image with no motion artifacts. Cardiac CT does not suffer from this inverse relationship, and allows for both high spatial and temporal resolution simultaneously. Electron beam CT (EBCT –described in detail in text to come) allows for high resolution imaging at 50–100 milliseconds ms. Multidetector CT; MDCT, with improved spatial resolution, allows for rotation speeds now on the order of 260–350ms. The most distinct advantage of cardiac CT over cardiac MR is the improved spatial resolution and thinner slice thickness achievable with current systems. CT has the ability to image every 0.5 mm (submillimeter slices), providing high z-axis (through plane resolution). In-plane resolution is dependent upon the number of pixels that can be seen by a given detector array. Resolution of current CT systems uses a matrix of 512×512, allowing x- and y-axis(in plane) resolution down to 0.35 mm. MR systems use a matrix of 256 × 256, and flat plate technology currently used in advanced fluoroscopy labs and cardiac catheterization labs use 1,024×1,024 matrix resolution. The best resolution reported by a cardiac MR study (using the 3Tesla magnet) demonstrated resolution in the x-, y- and z-axes of 0.6×0.6×3mm. The best resolution offered by cardiac CT is 0.35×0.35×0.5 mm, which is almost a factor of 10 better spatial resolution and approaching the ultimate for 3D tomography of nearly cubic (isotropic))"voxels" – or volume elements (a 3D pixel). As we consider noninvasive angiography with either CT or MR, we need to remember that both spatial and temporal resolution is much higher with traditional invasive angiography. Reconstruction algorithms and multi-"head" detectors common to both current electron beam and spiral/helical CT have been implemented

enabling volumetric imaging, and multiple high-quality reconstructions of various volumes of interest can be done either prospectively or retrospectively, depending on the method. The details of each type of scanner and principles of use will be described in detail.

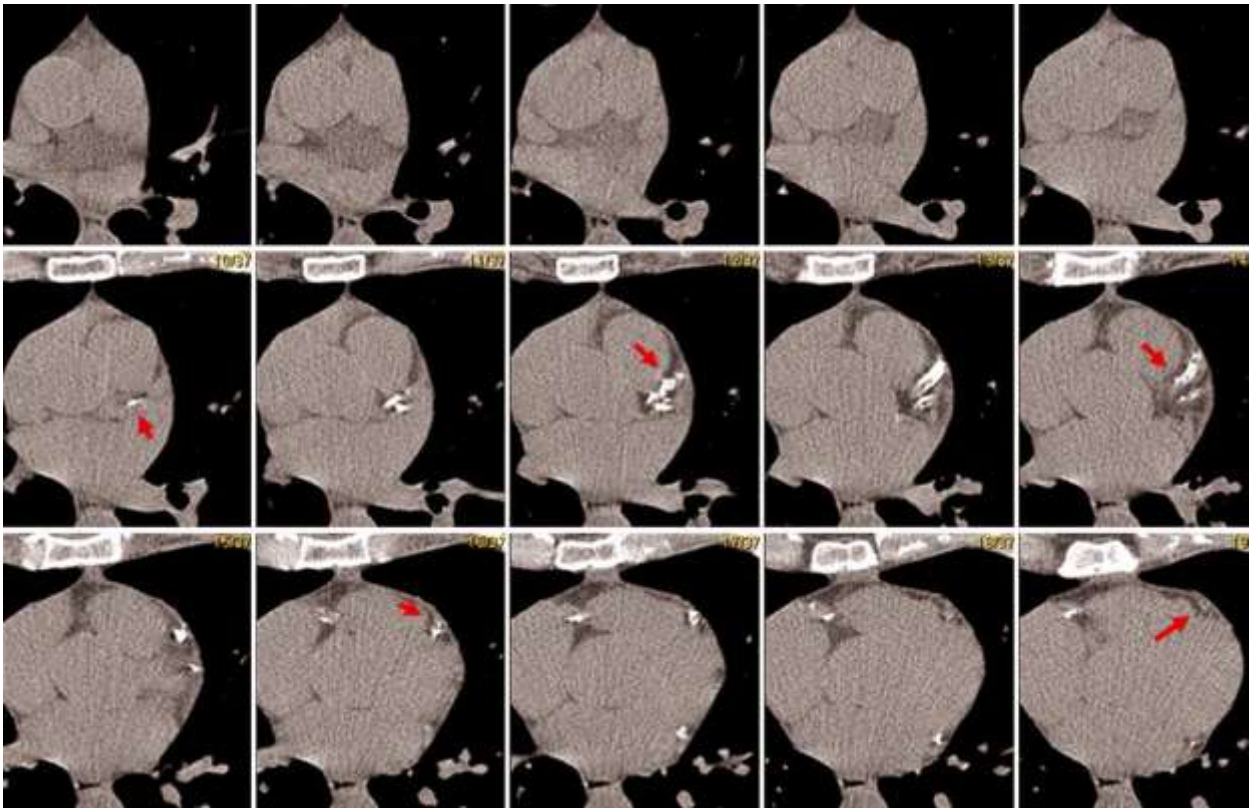

Figure 2.5. Sequential 3 mm slices from a non-contrast CT scan study (calcium scan). This study depicts the course and calcifications of the left anterior descending (LAD) artery. The white calcifications are easily seen (red arrows) and quantitated by the computer to derive a calcium score, volume or mass with high inter-reader reproducibility. (Budoff et.al (2010)).

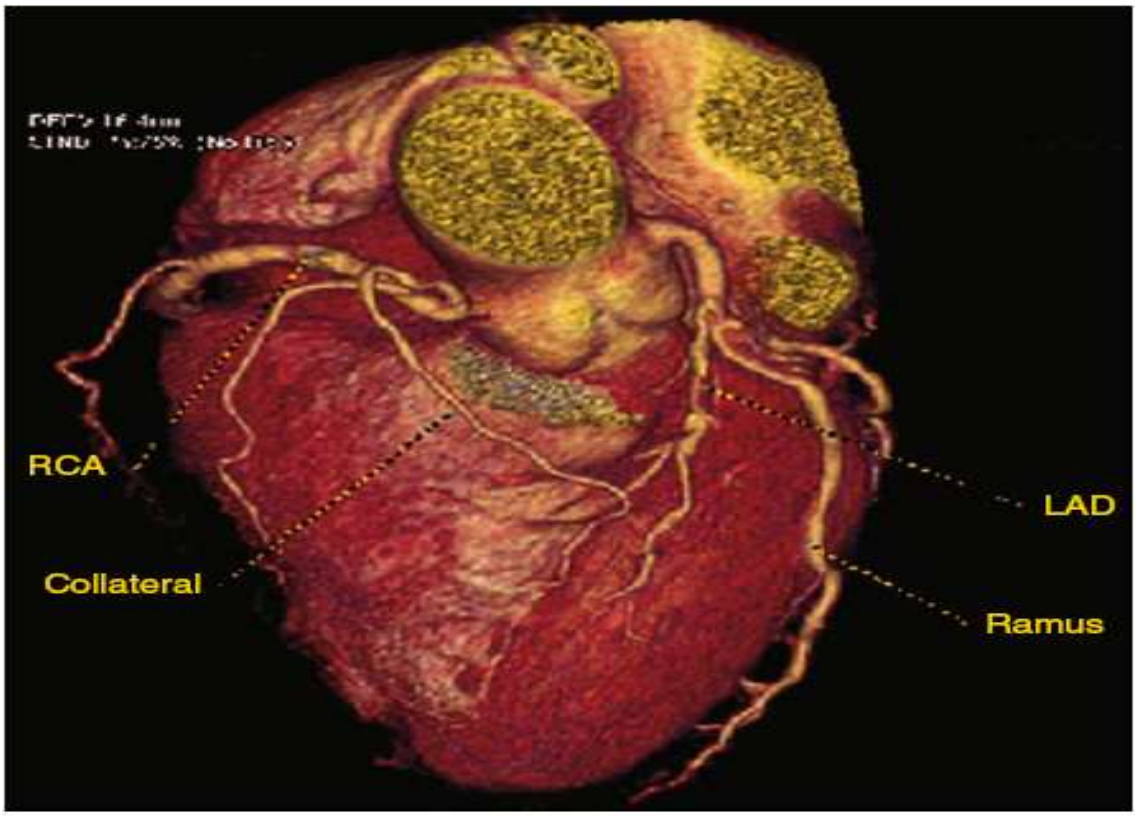

Figure 2.6. A contrast-enhanced CT of the coronary arteries, with excellent visualization of a high grade stenosis in the mid-portion of the LAD.

For above image a large collateral vessel is seen from the RCA, but this is quite rare, as usually the collaterals are too small to be well seen on cardiac CT. A large ramus intermedius is well visualized, and the dominant RCA is present. This is but one view of many that can be visualized with cardiac CT, allowing for near-complete visualizations of the coronary tree. Budoff et.al (2010).

Sample protocols for MDCT angiography: contrast-enhanced retrospectively ECG-gated scan as follow: 4-Slice scanner: 4×1.0 mm collimation, table feed 1.5 mm/rotation, effective tube current 400 mAs at 120 kV. Pitch = 1.5/4.0 collimation = 0.375. Average scan time = 35 s, 16-Slice scanner (1.5 mm slices): 16 × 1.5 mm collimation, table feed 3.8 mm/rotation, effective tube current 133 mAs at 120 kV. Pitch = 3.8/24 mm collimation = 0.16. Average scan time = 15–20 s, 16-Slice scanner (0.75 mm slices): 16 slices 0.75 mm collimation, table feed 3.4 mm/rotation,

effective tube current 550–650 mAs at 120 kV. Pitch = 3.4/12 mm collimation = 0.28. Average scan time = 15–20 s. 64-Slice scanner (0.625 mm slices): 64 slices 0.6.25 mm collimation, table feed 10 mm/rotation, effective tube current 685 mAs at 120 kV. Pitch = 10/40 mm collimation = 0.25. Average scan time = 5 s, Dual source scanner (0.6 mm slices): 32 × 0.6 mm collimation, table feed 6 mm/rotation, effective tube current 685 mAs at 120 kV. Pitch = 6/19.2 mm collimation = 0.3. Average scan time = 10–12 s, 320-Slice scanner (0. 5 mm slices): 320 × 0.5 mm collimation, table feed 12 mm/rotation, effective tube current 685 mAs at 120 kV. Pitch = 12/40 mm collimation = 0.3. Average scan time= 2–3s. (Budoff et.al (2010)).

2.3.1. MDCT Terminology:

2.3.1.1. Isotropic Data Acquisition.

The biggest advance that the newest systems provide is thinner slices, important for improving image quality as well as diminishing partial volume effects. The current systems allow for slice thick-nesses between 0.5 and 0.625 mm (depending on manufacturer and scan model). Thus, the imaging voxel is virtually equal in size in all dimensions (isotropic). The spatial resolution of current CT systems is 0.35 × 0.35 mm, and has always been limited by the z-axis (slice thickness). Current systems theoretically allow for isotropic resolution (as reconstructed images can be seen at 0.4 mm), allowing for no loss of data by reconstructing the data in a different plane. This is very important for imaging the coronary, peripheral, and carotid arteries, as they run perpendicular to the imaging plane – each slice only encompasses a small amount of data – and to follow these arteries, one must add multiple slices together in the z-axis. The old limitations of CT (better interpretation for structures that run within the plane it was imaged, i.e., parallel to the imaging plane) are no longer present. There is now no loss of data with reformatting the data with multi-planar reformation MPR or volume rendering VR. This differs significantly from MR, which due to thick slice acquisition (still >1 mm), does not

allow free rotation of the resultant in-plane images. Thus, acquisition for CT is quite simple, obtaining axial slices through the area of interest, with the ability to reconstructed 3D image that can be freely rotated.

2.3.1.2. Field of View:

Another method to improve image quality of the CT angiograph (CCTA) is to keep the field of view small. The matrix for CT is 512 × 512, meaning that there are 512 voxels in the x and y plane for a given field of view. If the field of view is 15 cm (small enough to encompass the whole heart, but only allows visualization of perhaps 4% of the lung field on average), than each pixel is 0.3 mm, which maximizes the spatial resolution of the current detector systems. Increasing the field of view to 45 cm (typical for encompassing the entire chest) increases each pixel dimension to 0.9 mm, effectively reducing the spatial resolution of each data-point 3-fold. Thus, there is a strong need to keep the field of view small, to both improve spatial resolution of the resultant image for interpretation, and decrease liability by having less lung, breast, and bone visualized on the interpreted scan. This is significantly better than current MR scanners (which utilize a 256×256 matrix), effectively50% the spatial resolution compared to CT for each the x and y plane. Current flat plate technology for fluoroscopy allows for 1,024×1,024 resolution, 2-fold better than CT and 4-fold better than MR in each plane. Budoff et.al (2010).

2.3.1.3. Contrast:

Finally, the high scan speed allows substantial reduction in the amount of contrast material. The high speed of the scan allows one to decrease the amount of contrast administered; by using a 64-channel unit with a detector collimation of 0.625 mm and a tube rotation of 0.35 s (typical values for a 64-detector CCTA), the acquisition interval is around 5–6 s, which allows one to reduce the contrast load to approximately 50mL. For a faster acquisition protocol, the contrast delivery strategy needs to be optimized according to the scan duration time. Use of a 320 detector

scanner (which currently has 0.5 mm slices), covers the entire heart with one rotation, further reducing the contrast needs (although some minimal amount of contrast will be required to fill the heart and arteries in question). The general rule is the duration of scanning (scan acquisition time) equals the contrast infusion. So, if an average rate of 5 mL/s is used, a15-s scan acquisition (typical 16 slice scanner) would require75 mL of contrast. With volume scanners (64+ detector systems), the scan times are reduced to 2–6 s, and contrast doses are subsequently reduced as well.

2.3.1.4. Slip Ring:

Allows continuous imaging, by transmitting power to the rotating frame from the stationary frame, and acquiring scan data, and allowing the gantry to rotate continuously as signals are received from the detector array DAS assembly, and then passes data from the rotating side to the stationary side of the slip ring.

2.3.1.5. X-ray Tube:

CT X-ray tubes are similar to conventional X-ray tubes, with some issues related to anode heat capacity and dissipation. More slices and higher mA capacity lead to more heat generation by the tube. The tube is limited by its capacity (how much heat a tube can store safely) and its dissipation (how fast the tube can cool down). Most systems use air cooling, while one uses water cooling to dissipate the heat.

2.3.1.6. Temporal Resolution:

When performing typical cardiac imaging, the temporal resolution of a MDCT system is proportional to the gantry speed, which determines the time to complete one 360° rotation. To reconstruct each slice, data from a minimum of 180° plus the angle of the fan beam are required (half scan reconstruction), typically 210° of the total 360° rotation. For a 16-row system with 0.40-s rotation, the temporal resolution is approximately 0.25 s or 250msfor a 50 cm display field of view. By reducing the display field of view to the 20 cm to encompass the heart, the number of views can be reduced to further improve temporal resolution to approximately 200ms per slice

(focusing on the central resolution of the image). The majority of MDCT systems currently have gantry speeds of 330–420ms and thus resultant temporal resolution of 180–300ms per image when used for measuring coronary calcium or creating individual images for CT angiography, as compared to 50–100ms for EBCT. The newest scanners now have rotation gantry speeds down to 270ms for a 360° rotation. Although physically faster rotational times may be possible in the future, this is still rotation of an X-ray source (with attached detectors) that must rotate around the patient. This is subject to the forces and limitations of momentum. It is estimated that a conventional CT system generates 18 G of force (18 times the force of gravity) and weighs over 1 ton currently. It is doubtful that great strides will be made on significantly faster rotation speeds, but with dual (and potentially more detector arrays), temporal resolution of cardiac CT may continue to improve. Budoff MJ et.al (2010).

2.3.1.7. Halfscan Reconstruction:

A multislice helical CT halfscan HS reconstruction algorithms most commonly employed for cardiac applications. Halfscan reconstruction theoretically uses scan data from a 180° gantry rotation (180–250ms) for generating one single axial image. However, more than50% of the scan is required to obtain the data for an individual slice. Most vendors report their half-scan acquisition times as 50% of their rotation speed (for example, a330ms scanner reporting temporal resolution of 165ms).Half of the rotation speed is the "central time resolution," or the time needed to create only the center of the image. In traditional or single-source systems, the single X-ray tube rotates around the patient opposite the detector array, allowing for images to be created continuously (thanks to the slip ring technology described earlier). Dual source scanners take two sets of images simultaneously, and "add" the data together, creating an image in half the required time (similar to multi-segment reconstruction described in text to come, available with single source scanners, but images are taken

over two successive heart beats instead of two sets of images acquired during the same heart beat). Either technique (multi-segment reconstruction or dual source imaging) effectively lowers the temporal resolution by a factor of two: thus, central time resolution drops from 165 to 83ms. MDCT using the standard halfscan reconstruction method permits reliable assessment of the main coronary branches (those in the center of the image field) in patients with heart rates below 70 beats/min. The necessity of a low heart rate is a limitation of MDCT coronary angiography using this methodology. With halfscan reconstruction, the proportion of the acquisition time per heartbeat is linearly rising from 20%at 60 beats/min to 33% at 100 beats/min. When evaluating the diastolic time, the proportion is much greater. Slower heart rates have longer diastolic imaging. The diastolic time useful for imaging for a heart rate of 60 beats/min is on the order of 500ms (excluding systole and atrial contraction).Thus, a 250ms scan will take up 50% of the diastolic imaging time. Increase the heart rate to 100 beats/min (systole remains relatively fixed) and the biggest change is shortening of diastole. Optimal diastolic imaging times are reduced to approximately 100ms, clearly far too short for a motion-free MDCT scan acquisition of 250ms Thus, heart rate reduction remains a central limitation for motion-free imaging of the heart using MDCT. This can be partially overcome by multi-segment reconstruction, described in text to come.

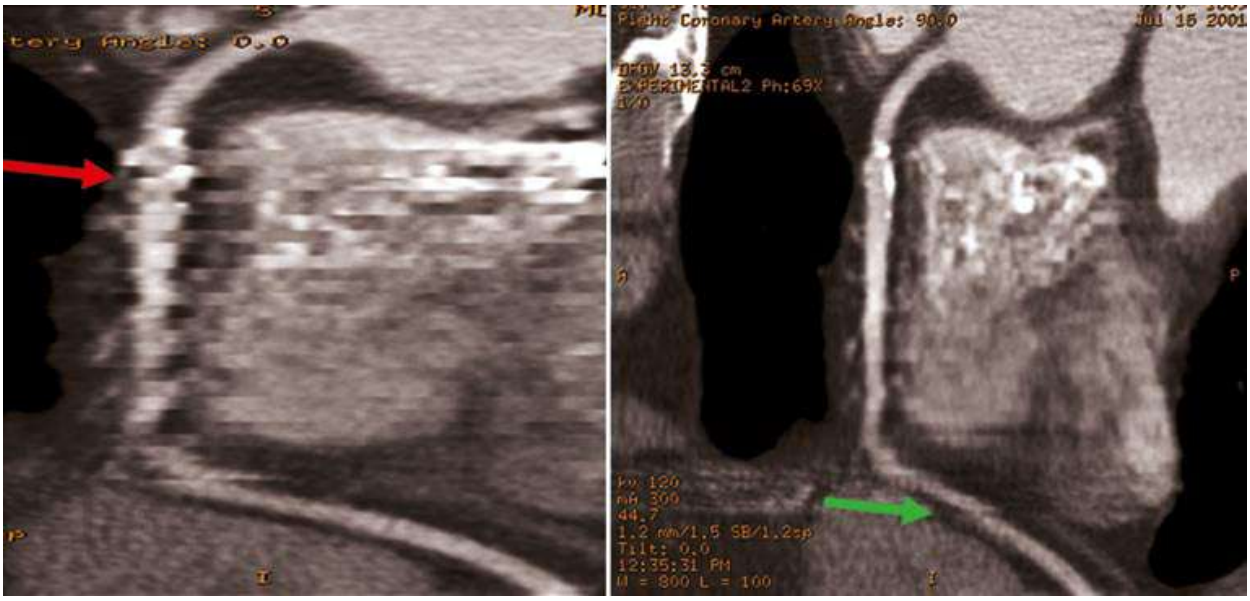

Figure 2.7. Light Speed-16 CT angiography images.

On the left is the halfscan reconstruction. On the right is a reconstructed image using the same dataset, using multi-segment reconstruction? There are still some motion artifacts in the distal right (green arrow), but much improved over the halfscan image, which is not interpretable (left side image arrow).

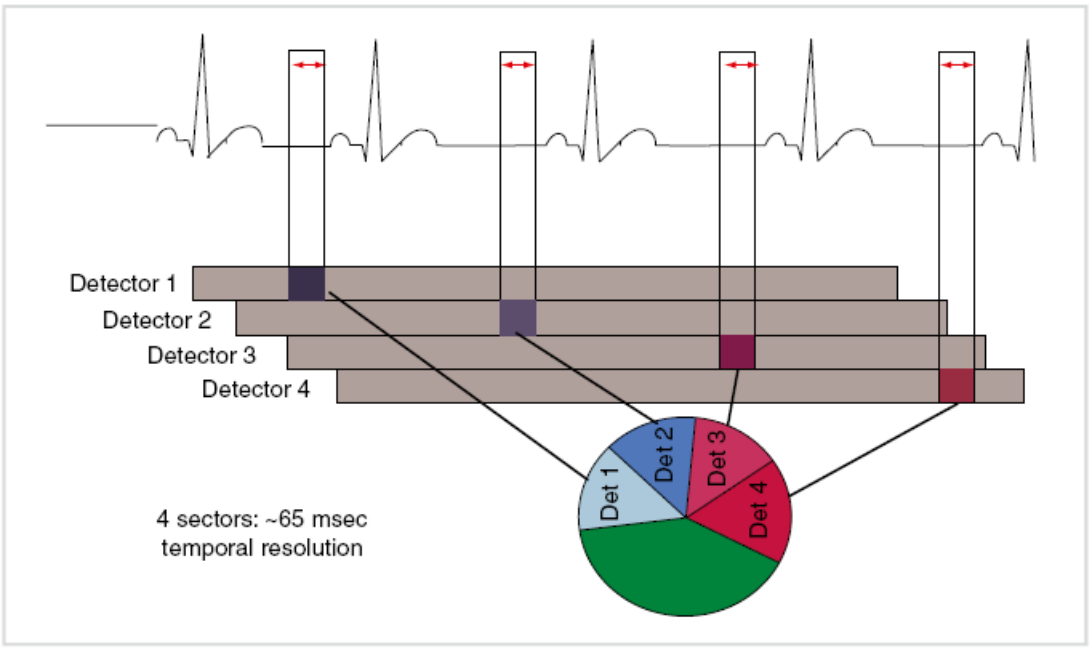

Figure 2.8. A demonstration of a theoretical image using multi-segment reconstruction.

The resulting image is constructed of four equal segments from four different detectors. Each is reconstructed from the same point in the cardiac cycle (approximately 50% in this depiction). Four different detectors, each visualizing the same portion of the heart in the same portion of the cardiac cycle, can be used to add together to create one image. In practice, the segments are not always of equal length, and four images are not always avail-able for reconstruction. Budoff MJ et.al (2010).

2.3.1.8. Retrospective Gating:

The ECG is used to add R peak markers to the raw data set. A simultaneous ECG is recorded during the acquisition of cardiac images. The ECG is retrospectively used to assign source images to the respective phases of the cardiac cycle (ECG gating). The best imaging time to minimize coronary motion is from 40 to 80% of the cardiac cycle (early to mid-diastole). The interval between markers determines the time of each scanned cardiac cycle. Retrospective, phase-specific, short time segments of several R-R intervals are combined to reconstruct a "frozen axial slice." During helical scanning, the patient is moved through the CT scanner to cover a body volume (i.e., the heart). An advantage of the helical acquisition mode is that there is a continuous model of the volume of interest from base to apex, as opposed to the sequential/cine mode in which there are discrete slabs of slices which have been obtained in a "step and shoot" prospective fashion. The obvious detriment to the helical acquisition is the increase in radiation dose delivered to the patient, as continuous images are created, and then "retrospectively" aligned to the ECG tracing to create images at any point of the R-R interval (cardiac cycle).

2.3.1.9. Prospective Triggering:

The prospectively triggered image uses a "step and shoot" system, similar to EBCT. This obtains images at a certain time of the cardiac cycle, which can be chosen in advance, and then only one image per detector per cardiac cycle is obtained. This greatly reduces radiation dose, as the scanner is not on continuously (such as

retrospective gating above). This has been used for quite a while with coronary calcium scanning, as multiple phases were not required to derive a calcium score. Only recently has this allowed for CT angiographic images, as there is markedly less data available to perform reconstructions. With retrospective gating, thousands of images are obtained as the detectors continuously acquire data. The resultant images are then 'retrospectively' aligned with the ECG, to create multiple datasets at each portion of the cardiac cycle. With prospective imaging, only images at a certain phase (for example 70% of the R-R interval, or mid-diastole) would be obtained, and then the scanner would move the patient (step), await another heart beat (R wave), and then trigger again (shoot) at 70%to obtain another set of images (64 images with a 64MDCT). This would continue for 3–5 beats until the entire heart is covered. With 320 detector scanners, the volume is covered within 1 heartbeat, at the predetermined phase, saving possible reconstruction artifacts when lining up volumes of data from subsequent heart beats (step or collimation artifacts). However, motion artifacts can still occur with more detector arrays, as the motion of the right coronary artery is dependent on the rotation speed (temporal resolution), not the number of detectors.

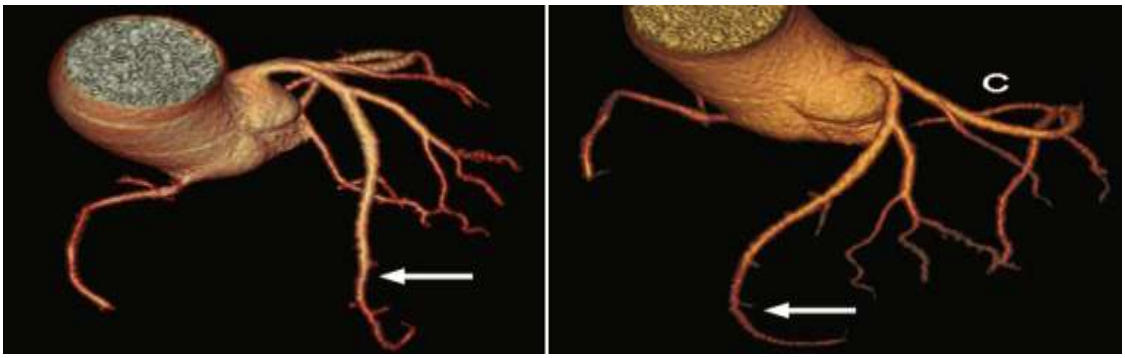

Figure 2.9. A contrast-enhanced CT angiogram demonstrating long segments of the LAD (arrow). Images such as seen here can be created which are much more similar to a conventional coronary angiogram, if desired.

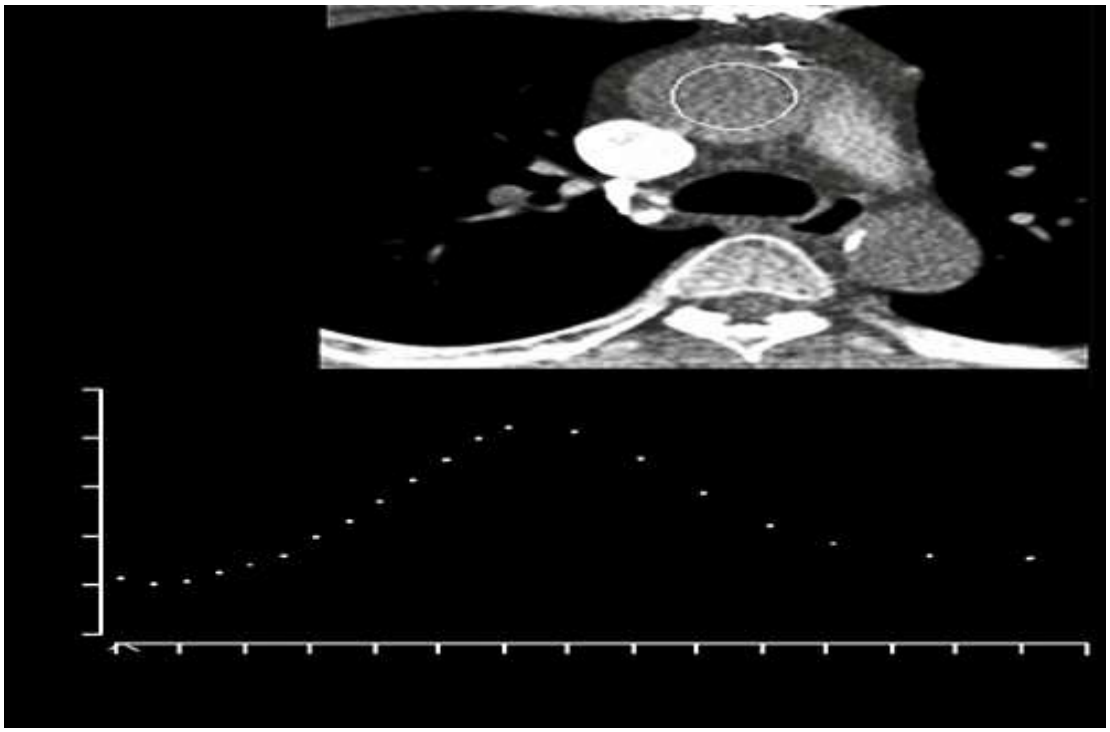

Figure 2.10. A flow or timing study. This study images the same level over time. A region of interest (in this study, the circle is placed in the ascending aorta) defines the anatomy to be measured.

The graph below measures the Hounsfield units (HU) of that region of interest on each subsequent image. Initially, there is no contrast enhancement, and the measures are of non-enhanced tissue, around 50–60 HU. Contrast starts to arrive on this study around 16 s, and peaks at 22 s. The bright white structure next to the ascending aorta is the superior vena cava, filled with unmixed contrast. Budoff MJ et.al (2010).

2.3.2. Radiation dose:

This section will briefly give the amount of radiation dose for each CT test.

Table 2.1 Common tests with estimated radiation exposures

Test	Radiation dose (mSv)	
1 Stress MIBI	9 (technetium), 41 (thallium)	
1 LC spine	1.3	
1 Barium enema	7	
1 Upper GI	3	
1 Abdominal X-ray	1	
1 Dental X-ray	0.7	
1 Cardiac catheterization	2.5–10	
	Radiation dose for MDCT (mSv)	Radiation dose for EBC (mSv)
Calcium scan	1–1.5	0.6
CT angiography	8–13	1–1.5
CCTA, prospective triggering	2–4	–
Lung CT	8	1.5
Abdomen/Pelvis	10	2
Body scan	12	2.6
Virtual colon	8–14	2–3

2.3.3. Clinical Applications of Cardiovascular CT:

The presence of coronary calcium is invariably an indicator of atherosclerosis (budoff MJ et.al (2009)), (blankenhorn et.al (1961)). Non-contrast studies can accurately identify and quantify coronary calcification (a marker of total plaque burden) Breen JF et.al 1992, while contrast-enhanced studies can define ventricular volumes, ejection fraction, and wall motion and wall thickening with high accuracy Lipton MJ et.al 1985. Studies can be performed at rest, and during exercise can identify reversible ischemia, (Wu YW et.al (2008)). Coronary angiography during cardiac catheterization is the clinical gold standard for definitive diagnosis and determination of coronary lesions. Pathologic studies have demonstrated that the severity of coronary stenosis is underestimated by visual analysis during clinical coronary angiography, (lessck J et.al (2007)–mintz GS (1995)). This may result from the limitations of resolution based upon fluoroscopy and the 2D imaging inherent in coronary angiography, as well as the inability to see beyond the lumen with conventional angiography. The true promise of cardiovascular CT is to visualize the coronary artery, including the lumen and wall. Three-dimensional digital coronary

images may provide more accurate representation of coronary artery anatomy and be more amenable to quantitation, thereby improving the diagnosis and treatment of CAD. There is rapidly accumulating data with both MDCT and EBCT to visualize the coronary arteries accurately and reliably (CT angiography).

Looking beyond the lumen by visualizing the wall and its constituents (including fat, calcium, and fibrous tissue) is now possible with cardiac CT. Coronary plaque composition evaluation is being actively investigated. This so-called "soft plaque" evaluation may prove to have prognostic significance over coronary calcium or risk factors alone, as well as helping to target revascularization better than luminography alone.

2.3.4. Interpretation, Prognostic Value, and Relationship to Lipids and Other Cardiovascular Risk Factors

CAC is pathognomonic for atherosclerosis, (blankenhorn et.al 1959-wexler L et.al 1996. Mönckeberg's calcific medial sclerosis does not occur in the coronary arteries faber et.al 1912) atherosclerosis is the only vascular disease known to be associated with coronary calcification. Calcium phosphate (in the hydroxyapatite form) and cholesterol accumulate in atherosclerotic lesions.

Circulating proteins that are normally associated with bone remodeling play an important role in coronary calcification, and arterial calcium in atherosclerosis is a regulated active process similar to bone formation, rather than a passive precipitation of calcium phosphate crystals, (bostrom K 1993. Rumberger et al. 1995). demonstrated that the total area of coronary artery calcification is highly correlated ($r = 0.9$) in a linear fashion with the total area of coronary artery plaque on a segmental, individual, and whole coronary artery system basis, and the areas of coronary calcification comprise approximately one-fifth that of the associated coronary plaque. Additionally, there were plaque areas without associated coronary calcium, suggesting that there may be a coronary plaque size most commonly

associated with coronary calcium but, in the smaller plaques, the calcium is either not present or is undetectable. Intravascular ultrasound, (baumgart D et.al 1997). Measures of combined calcified and non-calcified plaque confirm the strong relationship. Budoff MJ et.al (2010).

2.3.4.1. Technical methods:

Until recently, the data substantiating the importance of CAC have been derived almost exclusively through the use of electron beam tomography (EBT), utilizing a rotating electron beam to acquire prospectively triggered, and tomographic100-ms X-ray images at 3 mm intervals in the space of a 30- to 40-s breath hold. The multi-detector computed tomography MDCT technology is a more recent development and employs a rotating gantry with a special X-ray tube and variable number of detectors (from 4 to 64), with 165–375-ms images at 0.5, 1.5, 2.0, or 3.0 mm intervals, depending on the protocol and manufacturer.

2.3.4.2. Scoring

The presence of coronary calcium is sequentially quantified through the entire epicardial coronary system. Coronary calcium is defined as a lesion above a threshold of 130Hounsfield units (which range from −1,000 (air), through 0 (water), and up to +1,000 (dense cortical bone)), with an area of three or more adjacent pixels (at least 1 mm2). The original calcium score developed by Agatston AS et.al 1990. Is determined by the product of the calcified plaque area and maximum calcium lesion density (from 1 to 4 based upon Hounsfield units). Standardized categories for the calcium score have been developed with scores of 1–10 considered minimal, 11–100 mild, 101–400 moderate, and >400 severe. Examples are shown in Figure 4.1. The calcium volume score, callister et.al 1998. Is a more reproducible parameter that is independent of calcium density and is considered to be the parameter of choice for serial studies to track progression or regression of atherosclerosis? Phantom-based calcium mass scores are being developed that will be applicable to any CT

scanner becker CR et.al 2001, but have yet to be validated. Examples of CAC scans are shown in figure below

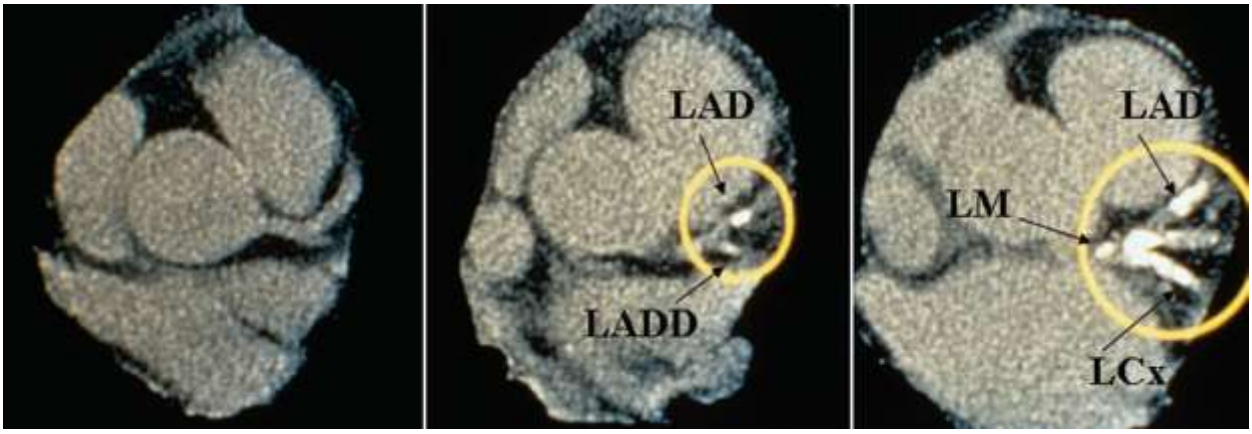

Figure 2.11. Examples of EBT coronary artery calcium (CAC) scans. Left: Normal without CAC. Center: Moderate CAC involving the left anterior descending (LAD) and circumflex (LCx) coronary arteries. Right: Extensive CAC involving the left main (LM), anterior descending, and circumflex coronary arteries.

2.3.4.3. Zero Coronary Artery Calcium Scores

Individuals with zero CAC scores have not yet developed detectable, calcified coronary plaque but they may have fatty streaking and early stages of plaque. Non-calcified plaques are present in many young adults. Nonetheless, the event rate in patients with CAC score 0 is very low raggi P et.al 2000, Greenland P et.al 2004, arad et.al 2005. Raggi et al. 2000, demonstrated an annual event rate of 0.11% in asymptomatic subjects with 0 scores (amounting to a 10-year risk of only 1.1%), and in the St Francis Heart Study arad Y et.al 2005, scores of 0 were associated with a 0.12% annual event rate over the ensuing 4.3 years. Greenland et al. 2005, in a higher-risk asymptomatic cohort, noted a higher annual event rate (0.62%) with 0 CAC scores; a less sensitive CAC detection technique and marked ethnic heterogeneity may have contributed to their findings, budoff MJ et.al 2000. In the definitive MESA study, 0 CAC was associated with a 0.11% annual event rate. In a meta-analysis of 64,873 patients followed for 4.2 years, the coronary event rate was

0.13% per year in the 25,903 patients with 0 CAC compared to 1% per year for the 42,283 with CAC > 0. In an analysis of all-cause mortality in 44,052 asymptomatic patients followed for 5.6 years, the deaths/1,000 patient years for the 19,898 with 0 CAC was 0.87, compared to 1.92 for CAC 1–10, and 7.48 for CAC > 10.While non-calcified, potentially "vulnerable" plaque is by definition not detected by CAC testing, CAC can identify the pool of higher-risk asymptomatic patients out of which will emerge approximately 95% of the patients presenting each year with sudden death or an acute MI. While the culprit lesion contains calcified plaque in only 80% of the acute events; Mascola A et.al 2000, of greater importance is the observation that exclusively soft, non-calcified plaque has been seen in only 5% of acute ischemic syndromes in both younger and older populations' Pohle K et.al 2003. In a more recent meta-analysis, only 2 of 183 (1.1%) 0 CAC patients were ultimately diagnosed with an acute coronary syndrome after presenting with acute chest pain, normal troponin, and equivocal EKG findings. CAC > 0 had 99% sensitivity, 57% specificity, 24% positive predictive value, and 99% negative predictive value for ACS. Thus, while it is uncommon that a patient with an imminent acute ischemic syndrome would have had a 0 CAC score, further evaluation, particularly with CCTA, is recommended.

2.3.4.4. Compliance with Therapeutic Interventions

With the exception of a single study flawed by insufficient power O'malley PG 2003, CAC has been shown to have a positive effect on compliance and initiation of and adherence to medication and life style changes. In 505 asymptomatic patients, statin adherence 3.6 years after visualizing their CAC scan was 90% in those with CAC > 400 compared to 75% for 100–399, 63% for 1–99, and 44% for 0 CAC ($p < 0.0001$). Similarly, in 980 asymptomatic subjects followed for 3 years, ASA initiation, dietary changes, and exercise increased significantly from those with 0 CAC (29, 33, 44%, respectively) and was lowest (29%) in those with CAC > 400

(61, 67, 56%, respectively orakzai RH et.al 2008. Finally, after a 6 year follow-up in 1,640asymptomatic subjects, the odds ratios for those with CAC > 0 compared to 0 CAC for usage of statins, ASA, and statin + ASA were 3.53, 3.05 and 6.97, respectively.

2.3.5. Coronary Artery Calcium and Guidelines:

Guidelines have been increasingly positive regarding the value of CAC scanning. The American College of Cardiology/American Heart Association expert consensus document (2000) concluded that: A negative EBCT test makes the presence of atherosclerotic plaque, including unstable plaque, very unlikely. A negative test is highly unlikely in the presence of significant luminal obstructive disease. Negative tests occur in the majority of patients who have angiographically normal coronary arteries. Firstly negative test may be consistent with a low risk of a cardiovascular event in the next 2–5 years. A positive EBCT confirms the presence of a coronary atherosclerotic plaque, secondly the greater the amount of calcium, the greater the likelihood of occlusive CAD, but there is not a 1-to-1 relationship, and findings may not be site specific. The total amount of calcium correlates best with the total amount of atherosclerotic plaque, although the true "plaque burden" is underestimated. A high calcium score may be consistent with moderate to high risk of a cardiovascular event within the next 2–5 years.

The American Heart Association Prevention V Update (2000) suggested that CAC be considered for risk assessment in the 6–20% Framingham 10-year risk category .The final report of the NCEP guidelines. Made the following recommendation on the basis of existing data at the time of publication (2002):

Therefore, measurement of coronary calcium is an option for advanced risk assessment in appropriately selected persons. In persons with multiple risk factors, high coronary calcium scores (e.g., >75th percentile for age and sex) denotes advanced coronary atherosclerosis and provides a rationale for intensified LDL-

lowering therapy. The European Guidelines on Cardiovascular Disease Prevention in Clinical Practice (2003) state "Coronary calcium scanning is thus especially suited for patients at medium risk," and use CAC to qualify conventional risk analysis de dadcer G et.al 2003. The American Heart Association Guidelines for Cardiovascular Disease Prevention in Women (2004) listed coronary calcification as an example of subclinical cardiovascular disease CVD placing patients in the10–20% Framingham 10-year risk category and acknowledged that "some patients with subclinical CVD will have>20% 10-year CHD risk and should be elevated to the high risk category" moscal et.al 2004. In 2006, the SHAPE guidelines. Recommended CAC or carotid intima-media thickening for all but the lowest risk asymptomatic men >45 and women >55 years, with subsequent treatment based upon the amount of CAC naghari M et.al 2006. Based upon the accumulated evidence at the time, which did not yet include the MESA, and Becker et.al 2003 data, the ACCF/AHA 2007 Clinical Expert Consensus Document judged that in the intermediate risk population "it may be reasonable to consider use of CAC measurement in such patients based on available evidence that demonstrates incremental risk prediction information in this selected (intermediate risk) patient group." A more robust endorsement is anticipated in future recommendations.

2.3.6. Calcium score related to its risk factor:

Conventional risk factors do correlate with CAC Kuller LH et.al 1999, even though CAC is superior to conventional risk factors in predicting outcomes. There is a clear association of CAC with a premature family history of CAD, diabetes, and lipid values in large groups of patients. However, the difficulty equating risk factors with CAC in individual patients has been highlighted by the work of Hecht et al in 930 consecutive primary prevention subjects undergoing EBT hect H et.al 2001. They found increasing likelihoods of CAC with increasing levels of low-density lipoprotein cholesterol (LDL-C) and decreasing levels of high-density lipoprotein

cholesterol (HDL-C) in the population as a whole, but found no differences in the amount of plaque between groups and demonstrated a total lack of correlation in individual patients between the EBT calcium percentile and the levels of total, LDL- and HDL-cholesterol, total/HDL-cholesterol, triglycerides, lipoprotein(a) (Lp(a)), homocysteine, and LDL particle size.

Postmenopausal women presented a striking example of the inability of conventional risk analysis to predict the presence or absence of subclinical atherosclerosis. There were no differences in any lipid parameters or in the Framingham Risk Scores between postmenopausal women with and without calcified plaque, rendering therapeutic decisions that are not plaque- imaging-based extremely problematic. Further support for the poor correlation of conventional risk factors with subclinical atherosclerosis was provided by Taylor et al in 630 active duty US Army personnel aged 39–45 years, undergoing EBT taylor et.al 2001. The area under the ROC curve was only 0.62 for the Framingham Risk Score and 0.61 for LDL-C alone. The authors conclude: "In this age homogeneous, low-risk screening cohort, conventional coronary risk factors significantly underestimated the presence of premature, subclinical calcified coronary atherosclerosis." These discrepancies underscore the difficulties inherent in applying population based guidelines derived from statistical analyzes to decision-making in the real world of individual patient care.

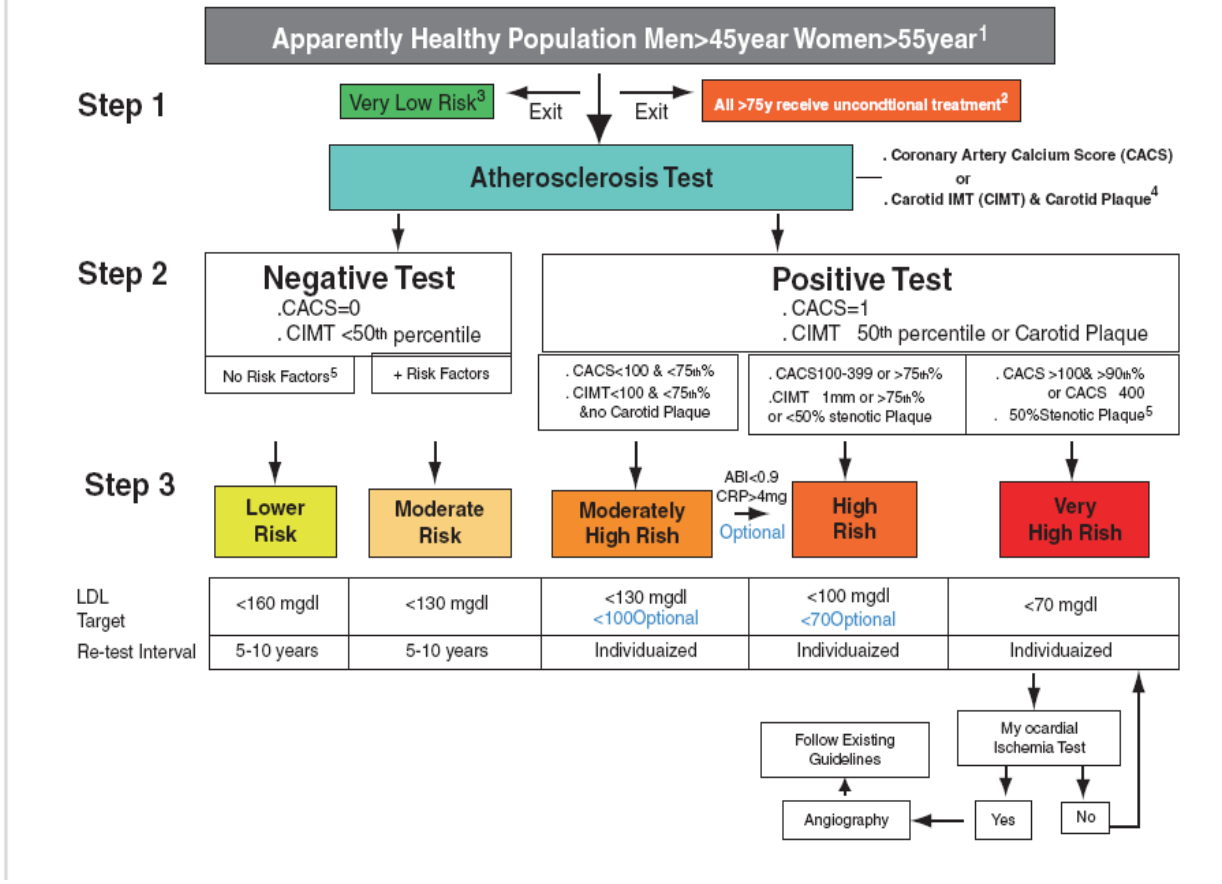

Figure 2.12. The SHAPE Guideline (towards the National Screening for Heart Attack Prevention and Education Program).

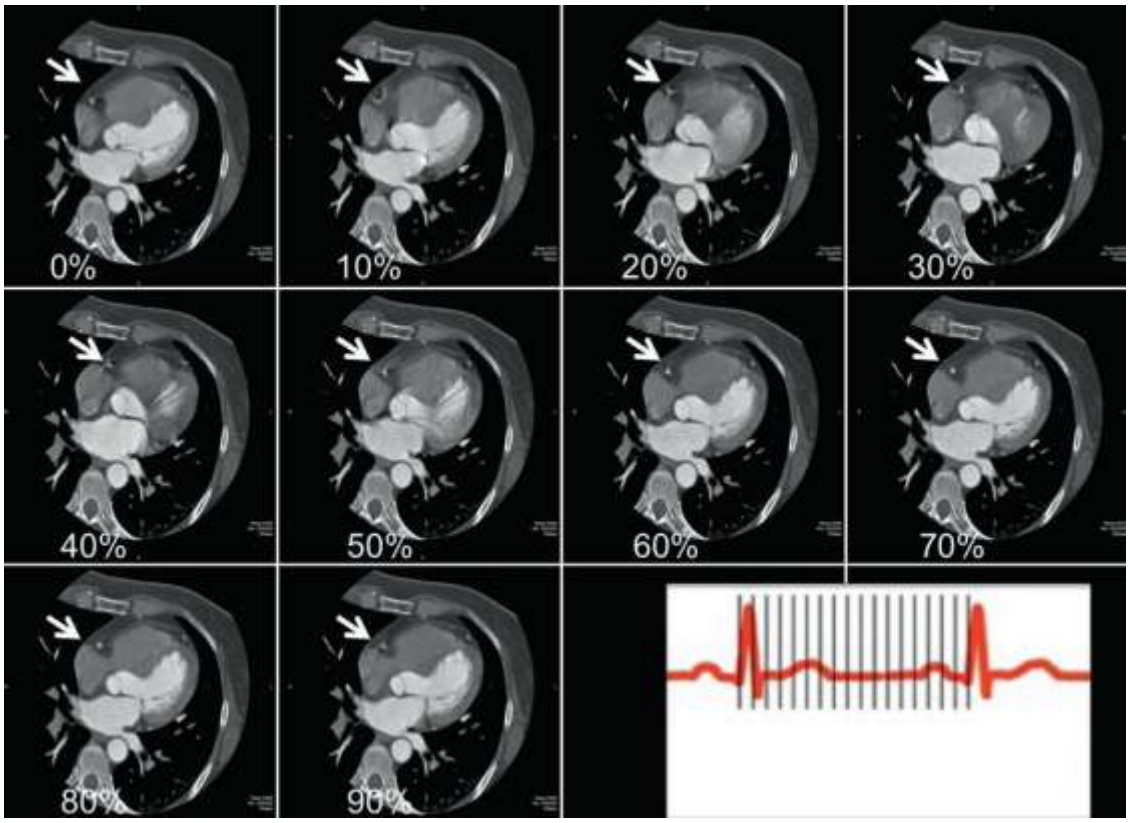

Figure 2.13. Demonstration of motion of the right coronary artery at serial decile percentages of the R-R interval during retrospective gating. The most optimal R-R percentage is 70%, as blurring of the right coronary artery is seen at other phases.

2.4. Previous study:

Efstathopoulos et.al (2009) aims to study the Reduction of the estimated radiation dose and associated patient risk with prospective ECG-gated 256-slice CT coronary angiography Computed tomography (CT) coronary angiography has been widely used since the introduction of 64-slice scanners and dual-source CT technology, but high radiation doses have been reported. Prospective ECG-gating using a 'step-and shoot' axial scanning protocol has been shown to reduce radiation exposure effectively while maintaining diagnostic accuracy. 256-slice scanners with 80 mm detector coverage have been currently introduced into practice, but their impact on radiation exposure has not been adequately studied. The aim of this study was to

assess radiation doses associated with CT coronary angiography using a 256-slice CT scanner. Radiation doses were estimated for 25 patients scanned with either prospective or retrospective ECG-gating. Image quality was assessed objectively in terms of mean CT attenuation at selected regions of interest on axial coronary images and subjectively by coronary segment quality scoring. It was found that radiation doses associated with prospective ECG-gating were significantly lower than retrospective ECG gating (3.2±0.6mSv versus 13.4 ± 2.7mSv). Consequently, the radiogenic fatal cancer risk for the patient is much lower with prospective gating (0.0176% versus 0.0737%). No statistically significant differences in image quality were observed between the two scanning protocols for both objective and subjective quality assessments. Therefore, prospective ECG-gating using a 'step-and shoot' protocol that covers the cardiac anatomy in two axial acquisitions effectively reduces radiation doses in 256-slice CT coronary angiography without compromising image quality.

McCullough et.al (2007) aims to study the coronary heart disease in general population and he was stated that, coronary heart disease is the most common cause of death in the general population and in patients with ESRD. The principles of cardiovascular risk assessment and management apply to both populations. Advances in noninvasive coronary artery imaging have improved early detection of subclinical disease. The goals of medical management of coronary disease are to modify the natural history of disease and to improve the symptoms of angina. Coronary revascularization poses a different risk and benefit equation in the ESRD population. In stable ESRD with multi-vessel coronary artery disease, coronary bypass surgery, despite the upfront risks of stroke, myocardial infarction, and chest wound infection, seems to be a favored approach. In patients with ESRD and acute coronary syndromes, percutaneous coronary intervention on the target vessel has

been associated with the most favorable outcomes. This article explores the clinical issues with respect to coronary artery disease in patients with ESRD.

Hamon et.al (2006) the aims of his study was designed to define the current role of multislice spiral computed tomography MSCT for the diagnosis of coronary artery disease CAD using a meta-analytic process. Multislice spiral computed tomography has recently been proposed as an alternative to conventional coronary angiography (CA) for the diagnosis of CAD. Using Medline, this study was identified 29 studies (2,024 patients) evaluating CAD by means of both MSCT (16 slices) and conventional CA before July 2006. After data extraction the analysis was performed according to a random-effects model. The main result of this study was: The per-segment analysis pooled the results from 27 studies corresponding to a cumulative number of 22,798 segments. Among unassessable segments, 4.2% were excluded from the analysis and 6.4% were classified at the discretion of the investigators, underscoring the shortcomings of MSCT. With this major limitation, the per-segment sensitivity and specificity were 81% (95% confidence interval [CI] 72% to 89%) and 93% (95% CI 90% to 97%), respectively, with positive and negative likelihood ratios of 21.5 (95% CI 13.1 to 35.5) and 0.11 (95% CI 0.06 to 0.21), respectively, and positive and negative predictive values of 67.8% (95% CI 57.6% to 78.0%) and 96.5% (95% CI 94.7% to 98.3%), respectively. As expected, the per-patient analysis has shown an increased sensitivity of 96% (95% CI 94% to 98%) but a decreased specificity of 74% (95% CI 65% to 84%).

Jakobs et.al (2002) he was aims to evaluate image quality and radiation exposure of retrospectively ECG-gated multislice helical CT MSCT investigations of the heart with ECG-controlled tube current modulation. One hundred patients underwent MSCT scanning (Somatom Volume Zoom, Siemens, Forchheim, Germany) for detection of coronary artery calcifications. A continuous helical data set of the heart was acquired in 50 patients (group 1) using the standard protocol with constant tube

current, and in 50 patients (group 2) using an alternative protocol with reduced radiation exposure during the systolic phase. The standard deviations SD of predefined regions of interest ROIs were determined as a measure of image noise and were tested for significant differences. There was no significant difference between group 1 and group 2 with respect to image noise. Radiation exposure with and without tube current modulation was 1.0 and 1.9mSv ($p<0.0001$), respectively, for males and 1.4 and 2.5mSv ($p<0.0001$), respectively, for females; thus, there was a mean dose reduction of 48% for males and45% for females, respectively. The ECG-controlled tube current modulation allows significant dose reduction when performing retrospectively ECG-gated MSCT of the heart.

KOPP et.al (2004) stated that in the last 2 years, mechanical multi-detector-row CT (MDCT) systems with simultaneous acquisition of four slices and a half second scanner rotation time have become widely available. Data acquisition with these scanners allows for considerably faster coverage of the heart volume compared with single slice scanning. This increased scan speed can be used for retrospective gating together with 1 mm collimated slice widths and allows coverage of the entire cardiac volume in one breath-hold. First results from studies in correlation with intracoronary ultrasound suggest that MDCT technology not only offers the possibility to visualize intracoronary stenosis non-invasively, but also to differentiate plaque morphology. This is especially the case with the next generation of 16-row MDCT systems. An increased number of simultaneously acquired slices and submillimeter collimation for cardiac applications allows true isotropic scanning with high temporal resolution. Contrast-enhanced MDCT is a promising non-invasive technique for the detection, visualization and characterization of stenotic artery disease. It could act as a gatekeeper prior to cardiac catherization and finally replace conventional diagnostic modalities.

Chao et.al (2010) aims to assess the diagnostic accuracy of 256-row computed tomographic angiography (CTA) in patients with suspected coronary artery disease (CAD). Non-invasive imaging of the coronary artery by CTA has increasingly been used in recent years. The accuracy of 256-row CTA has not yet been studied. We sought to assess the accuracy of 256-rowCTA compared with invasive coronary angiography (ICA) in the diagnosis and assessment of CAD. A prospective evaluation of 104 consecutive individuals who accepted CTA and then underwent ICA. The presence of stenosis ≥50% was considered obstructive. The diagnostic accuracy of CTA for detecting obstructive stenosis was compared with that of ICA. The area under the receiver-operating-characteristic curve (AUC) was used to evaluate the diagnostic accuracy of CTA relative to ICA. A total of 86 patients had obstructive CAD. The patient-based analysis of CTA for detecting stenosis ≥50% according to ICA revealed an AUC of 0.744 [95% confidence interval (CI), 0.572–0.916], with a sensitivity of 98.8%, a specificity of 50%, a positive predictive value (PPV) of 92.4%, and a negative predictive value (NPV) of 87.5%. The segment-based analysis revealed an AUC of 0.915 (95% CI, 0.847–0.982), with a sensitivity of 93.5%, a specificity of 95%, a PPV of 77.6%, and an NPV of 98.7%. The vessel-based analysis revealed an AUC of 0.887 (95% CI, 0.808–0.966), with a sensitivity of 94.3%, a specificity of 87.3%, a PPV of82.7%, and an NPV of 95.9%. A 256-Row CTA is a highly sensitive test of CAD and has a high predictive value. 256-Row CTA may be a potential alternative to detect coronary artery stenosis and rule out CAD in suspected patients.

Graaf et.al (2010) stated that the multi-detector computed tomography coronary angiography (CTA) has emerged as a feasible imaging modality for non-invasive assessment of coronary artery disease (CAD). Recently, 320-row CTA systems were introduced, with 16 cm anatomical coverage, allowing image acquisition of the entire heart within a single heartbeat. The aim of the present study was to assess the

diagnostic accuracy of 320-row CTA in patients with known or suspected CAD. A total of 64 patients (34 male, mean age 61+16 years) underwent CTA and invasive coronary angiography. All CTA scans were evaluated for the presence of obstructive coronary stenosis by a blinded expert, and results were compared with quantitative coronary angiography. Four patients were excluded from initial analysis due to non-diagnostic image quality. Sensitivity, specificity, and positive and negative predictive values to detect 50% luminal narrowing on a patient basis were 100, 88, 92, and 100%, respectively. Moreover, sensitivity, specificity, and positive and negative predictive values to detect 70% luminal narrowing on a patient basis were 94, 95, 88, and 98%, respectively. With inclusion of non-diagnostic imaging studies, sensitivity, specificity, and positive and negative predictive values to detect _50% luminal narrowing on a patient basis were 100, 81, 88, and 100%, respectively. The current study shows that 320-row CTA allows accurate non-invasive assessment of significant CAD.

Salm et.al (2006) aims to compare multi-detector row computed tomography (MDCT) global and regional left ventricular (LV) function assessment with echocardiography and cardiovascular magnetic resonance (CMR).Methods and results: In 25 patients, who were referred for noninvasive angiography with 16-detector row CT, LV function assessment was also performed. A subsequent echocardiogram was performed, and in a subgroup of patients, CMR examination was completed to evaluate LV function. For global function assessment, the LV ejection fraction (LVEF) was calculated. Regional LV function was scored using a 17-segment model and a 4-point scoring system. MDCT agreed well with echocardiography for the assessment of LVEF (rZ0.96; bias 0.54%; $p<0.0001$) and regional LV function (kZ0.78). Eight patients had no contra-indications and gave informed consent for CMR examination. A fair correlation between MDCT and CMR was demonstrated in the assessment of LVEF (rZ0.86; bias _1.5%; $p<0.01$).

Regional LV function agreement between MDCT and CMR was good (kZ0.86). Conclusion: MDCT agreed well with both echocardiography and CMR in the assessment of global and regional LV function. Global and regional LV function may accurately be evaluated by 16-detector row CT, and can be added to a routine CT image analysis protocol without need for additional contrast or imaging time.

Allister et.al (1998) stated that the angiographic studies of the regression of coronary artery disease are invasive and costly, and they permit only limited assessment of changes in the extent of atherosclerotic disease. Electron-beam computed tomography (CT) is noninvasive and inexpensive. The entire coronary-artery tree can be studied during a single imaging session, and the volume of coronary calcification as quantified with this technique correlates closely with the total burden of atherosclerotic plaque. A retrospective study of 149 patients (61 percent men and 39 percent women; age range, 32 to 75 years) with no history of coronary artery disease who were referred by their primary care physicians for screening electron-beam CT. All patients underwent base-line scanning and follow-up assessment after a minimum of 12 months (range, 12 to 15), and a volumetric calcium score was calculated as an estimate of the total burden of plaque. Treatment with 3-hydroxy-3-methylglutarylcoenzyme A (HMG-CoA) reductase inhibitors was begun at the discretion of the referring physician. Serial measurements of low-density lipoprotein LDL cholesterol were obtained, and the change in the calcium-volume score was correlated with average LDL cholesterol levels. One hundred five patients (70 percent) received treatment with HMG-CoA reductase inhibitors, and 44 patients (30 percent) did not. At follow up, a net reduction in the calcium-volume score was observed only in the 65 treated patients whose final LDL cholesterol levels were less than 120 mg per deciliter (3.10mmol per liter) (mean [±SD] change in the score, ¡7±23 percent; P=0.01). Untreated patients had an average LDL cholesterol level of

at least120 mg per deciliter and at the time of follow-up had significant net increase in mean calcium-volume score (mean change, +52±36 percent; P<0.001). The40 treated patients who had average LDL cholesterol levels of at least 120 mg per deciliter had a measurable increase in mean calcium-volume score (mean change, +25±22 percent, P<0.001), although it was smaller than the increase in the untreated patients. The extent to which the volume of atherosclerotic plaque decreased, stabilized, or increased was directly related to treatment with HMGCoA reductase inhibitors and the resulting serum LDL cholesterol levels. These changes can be determined noninvasively by electron-beam CT and quantified with use of a calcium-volume score.

George et.al (2012) stated that Coronary MDCT angiography has been shown to be an accurate noninvasive tool for the diagnosis of obstructive coronary artery disease (CAD). Its sensitivity and negative predictive value for diagnosing percentage of stenosis are unsurpassed compared with those of other noninvasive testing methods. However, in its current form, it provides no information regarding the physiologic impact of CAD and is a poor predictor of myocardial ischemia.CORE320 is a multicenter multinational diagnostic study with the primary objective to evaluate the diagnostic accuracy of 320-MDCT for detecting coronary artery luminal stenosis and corresponding myocardial perfusion deficits in patients with suspected CAD compared with the reference standard of conventional coronary angiography and SPECT myocardial perfusion imaging.

Earls et.al (2008) aims to retrospectively compare image quality, radiation dose, and blood vessel assess ability for coronary artery computed tomographic (CT) angiograms obtained with a prospectively gated transverse (PGT) CT technique and a retrospectively gated helical (RGH) CT technique. This HIPAA-compliant study

received a waiver for approval from the institutional review board, including one for informed consent. Coronary CT angiograms obtained with 64–detector row CT were retrospectively evaluated in 203 clinical patients. A routine RGH technique was evaluated in 82 consecutive patients (44 males, 38 females; mean age, 55.6 years). The PGT technique was then evaluated in 121 additional patients (71 males, 50females; mean age, 56.7 years). All images were evaluated for image quality, estimated radiation dose, and coronary artery segment assess ability. Differences in image quality score were evaluated by using a proportional odds logistic regression model, with main effects for three readers, two techniques, and four arteries. The mean effective dose for the group with the PGT technique was 2.8mSv; this represents an 83% reduction as compared with that for the group with the RGH technique (mean, 18.4mSv; P<.001). The image quality score for each of the arteries, as well as the overall combined score, was significantly greater for images obtained with PGT technique than for images obtained with RGH technique. The combined mean image quality score was 4.791 for images obtained with PGT technique versus 4.514 for images obtained with RGH technique (proportional odds model odds ratio, 2.8; 95% confidence interval: 1.7, 4.8).The percentage of assessable coronary artery segments was 98.6% (1196 of 1213) for images obtained with PGT technique versus 97.9% (1741 of 1778) for images obtained with RGH technique (P<0.83).

Chapter Three

Methodology

3.1. Material:

The study was executed using multi-detector computed tomography scanner MDCT64-Slice scanner (0.625 mm slices): 64 slice 0.6.25 mm collimation, table feed 10 mm/rotation, effective tube current 685 mAs at 120 kV. Pitch = 10/40 mm collimation = 0.25. Average scan time = 5 s, to scan the patient with coronary problems, with 64-slice (all machines), detector array, fan beam shape, CT monitor for controlling scanning and processing. Cardiac trigger monitor with electrode leads (3000 TOSHEIBA) to monitor the heart rate, contrast injector (Medrao Toshiba-2ways) for flush contrast media to patient and VITREA SYSTYM (TOSHIBA) for diagnosis images and reconstruction and volume rendered purposes.

3.2. Method:

In 101 patients (59 male, 42 female; mean age, 58.98 years) were included. MDCTA was performed. Patients with contraindications to iodinated contrast agent, and unstable clinical presentation, calcium scoring more than 1000, bypass surgery were excluded. The Research Counsel Board -College of Medical Radiological Science approved the research protocols. All patients underwent MDCTA of the coronary vessels by using a 64 row MDCT Toshiba system. Patients were placed in the supine position; Patients were also instructed not to breathe for 10-30 second during coronary artery angiography examination. Contrast medium was injected using power injector. Scanning started 5 seconds after enhancement in the aorta reached 60 HU. CT technical parameters included: matrix 512 X 512, field of view (FOV) 20 cm; tube current 685 mAs at 120kV; table feed 10mm/rotation, pitch 10/40mm. Axial images were analyzed. Cardiac trigger monitor with electrodes leads (3000

Toshiba) to monitor the heart rate, contrast injector (Medrao Toshiba) for flush contrast media to the patient and VITREA SYSTEM for diagnosis images and reconstruction and volume rendered purposes were used. For patient's preparation, caffeine and drugs that increases the heart rate were avoided prior to the cardiac CTA investigation. When β-blocker was used, patients with bronchial asthma, heart failure were contraindicated and have to be ruled out. In cases where the heart rate of the patients was above 60 bpm, the scan was not performed. Monitoring of vital function (heart rate) was checked. The patient's age, heart rate, and calcium score were evaluated, the arteries including left anterior descending artery (LAD), right coronary artery (RCA), left circumference artery (LCXR) were characterized for CAD according to the CT outcome. Plaques were characterized as (soft, mixed, calcified and non-calcified).

3.2.1. Study area:

This study was conducted at Khartoum state hospitals and diagnostic centers which was include diagnostic center at royal scan center, Alamal diagnostic center, the doctor specialized hospital.

3.2.2. Study duration:

This study was carried out from March 2014 to September 2015

3.2.3. The study population:

The study sample was consisted of (150-200) patient with CAD collected from three different diagnostic center as mentioned previously.

3.2.4. Study sample:

The study sample will consist of 150-200 patients with CAD.

3.2.5. Inclusion criteria:

The study will include all patients with CAD at age between (20-90years), female or male.

3.2.6. Exclusion criteria:

All patients with Allergy to contrast agent, Pregnancy, Renal insufficiency, bypass surgery and increasing of calcium score more than 1000 Agatston was excluded from this study and the patient with high heart rate and non-co-operative patient.

3.2.7. Statistical analysis:

All data were presented as mean± SD values. Data were analyzed by an independent t test and by correlation analysis with the use of the SPSS (Inc., Chicago, Illinois version 16). A value of $P<0.05$ was considered significant.

3.2.8. Method of data collection:

The data were collect on master data sheet from the diagnostic stations which was include all parameters need for evaluations.

3.2.9. Variables of the study:

Patient gender, Age, History of disease and Sign and symptoms, plaque type, degree of stenosis, and calcium score.

3.2.9.1. Example of standard master data sheet will be used in data collection

Age	Gender	Sign and symptom	Patient history	Heart rate	ECG finding	Echo finding	Lap investigation	Calcuim score	Affected artery	Degree of stenosis	Plaque type	Location of lesion	Paient result

3.2.10. Ethical issues:

- There was official written permission to Khartoum state diagnostic centers to take the data.
- No patient data were published also the data was kept in personal computer with personal password.

Chapter four

Table (4.1): Patients Demographic Data

Variables	Age/years	Heart rate/ bpm
Mean	58.98	63.03
Median	60.00	64.00
Std. Deviation	10.91	3.99
Minimum	10.00	52.00
Maximum	87.00	69.00
N	101	101

Table (4.2): Calcium Scoring (Agatston) in Coronary Arteries (LAD, RCA and LCFX)

Variables	LAD	RCA	LCFX
Mean	89.92	80.72	12.58
Median	0.00	0.00	0.00
Std. Deviation	255.60	367.64	58.25
Minimum	0.00	0.00	0.00
Maximum	1806.00	2918.00	508.00
N	101	101	101

Quantitative Coronary Angiography Calcium Values Based on Computed Tomography; RCA stands for Right Coronary Artery; LAD for Left Anterior Descending Artery and LCFX stands Left Circumflex Coronary Artery.

Table (4.3): Plaque type, frequency and percentages

Plaque type		
Variables	**Frequency**	**Percentages%**
Calcified	30	29.7
Mixed	9	8.9
Non Calcified	11	10.9
Soft	1	1.0
Normal	50	49.5
Total	101	100.0

Table (4.4): Distribution of Coronary Plaques

Coronary Artery Lesions Site	**Frequency**	**Percentages (%)**
Proximal	16	15.8
Middle	20	19.8
Distal	5	5.0
Proximal &Middle	4	4.0
Proximal & Distal	3	3.0
Middle & Distal	3	3.0
Normal	50	49.5
Total	101	100.0

Table (4.5): Descriptive Findings of Coronary Arteries with Correlation to Calcium Scoring (Agatston Values)

Descriptive findings of coronary arteries with correlation to calcium scoring						
Variables		**N**	**Mean**	**STDV**	**Min**	**Max**
LAD Left Anterior Descending Artery	Mild atherosclerosis	11	6.8	16.2	0.0	51.0
	Moderate atherosclerosis	2	0.0	0.0	0.0	0.0
	Severe atherosclerosis	2	174.0	243.2	2.0	346.0
	Mild Stenosis	17	177.4	242.7	31.0	619.0
	Severe Stenosis	10	415.4	573.9	13.0	1806.0
	Severe Calcification	2	669.0	483.7	327.0	1011.0
	Total Occlusion	2	83.5	118.1	0.0	167.0
	Pericarditis	2	146.0	0.0	146.0	146.0
	Normal	53	4.9	13.1	0.0	67.0
	Total	101	89.9	255.6	0.0	1806.0
P value	Correlations are significant at P<0.000 p=0.000					
RCA Right Coronary Artery	Mild atherosclerosis	11	13.5	13.7	0.0	31.0
	Moderate atherosclerosis	2	0.0	0.0	0.0	0.0
	Severe atherosclerosis	2	81.0	114.6	0.0	162.0
	Mild Stenosis	17	145.6	600.6	0.0	2017.0
	Severe Stenosis	10	260.0	315.6	0.0	1011.0

	Severe Calcification	2	1484.0	2027.9	50.0	2918.0
	Total Occlusion	2	1.5	2.1	0.0	3.0
	Pericarditis	2	1.0	0.0	1.0	1.0
	Normal	53	2.2	7.4	0.0	31.0
	Total	101	80.7	367.6	0.0	2918.0
P Value	Correlations are significant at P<0.000 p=0.000					
LCFX Left Circumflex Coronary Artery	Mild atherosclerosis	11	0.9	2.7	0.0	9.0
	Moderate atherosclerosis	2	0.0	0.0	0.0	0.0
	Severe atherosclerosis	2	3.5	4.9	0.0	7.0
	Mild Stenosis	17	36.6	8299	0.0	268.0
	Severe Stenosis	10	76.3	160.9	0.0	508.0
	Severe Calcification	2	7.0	5.7	3.0	11.0
	Total Occlusion	2	3.5	4.9	0.0	7.0
	Pericarditis	2	80.0	0.0	80.0	80.0
	Normal	53	0.6	2.3	0.0	11.0
	Total	101	12.6	58.3	0.0	508.0
P Value	Correlations are significant at P<0.000 p=1.000					

Table (4.6) Calcium Score Values and Plaque Types.

CALCIUM SCORE VALUES AND PLAQUE TYPE						
		N	Mean	STDV	Min	Max
LAD Left Anterior Descending Artery	Calcified	30	205.66	390.40	0.00	1806.00
	Normal	50	19.34	103.72	0.00	730.00
	Mixed	9	123.44	228.11	0.00	538.00
	Non Calcified	11	75.81	223.26	0.00	747.00
	Soft	1	0.00	0.0	0.00	0.00
	Total	101	89.92	255.60	0.00	1806.00
P Value	Correlation is significant at p<0.005 p=0.033					
RCA Right Coronary Artery	Calcified	30	186.13	556.77	0.00	2918.00
	Normal	50	1.96	6.79	0.00	31.00
	Mixed	9	10.44	11.79	0.00	25.00
	Non Calcified	11	215.81	602.31	0.00	2012.00
	Soft	1	3.0000	0.0	3.00	3.00

	Total	101	80.72	367.64	0.00	2918.00
P Value	Correlation is significant at p<0.005 p=0.156					
LCFX Left Circumflex Coronary Artery	Calcified	30	36.46	103.41	0.00	508.00
	Normal	50	1.88	8.01	0.00	40.00
	Mixed	9	2.22	3.99	0.00	11.00
	Non Calcified	11	5.09	11.92	0.00	40.00
	Soft	1	7.00	0.0	7.00	7.00
	Total	101	12.58	58.25	0.00	508.00
P Value	Correlation is significant at p<0.005 p=0.123					

Chapter five

Discussion, Conclusion and Recommendations

5.1. Discussion:

Multi detector row computed tomography angiography MDCTA recently emerged as a potential alternative to current imaging methods for the assessment of vessel structure and atherosclerotic plaque morphology of the coronary arteries [Kopp AF et al, 2002; Sato Y et.al 2003; Maruyama T et.al 2004; Matsuo S et.al 2004; Nieman K et.al 2002]

Our study was designed to evaluate the role of CTA in characterization of coronary arteries plaque .The study was obtained in 101 subjects with suspected to have coronary artery disease and were scanned for the first time by CT scan. Their mean age was 58.98years±10.9 and their mean heart rate was 63.03±3.99, this was presented in table (4.1).

Quantitative coronary angiography calcium values (CAC) based on computed tomography were obtained for (RCA), Left Anterior Descending Artery (LAD); Left Circumflex Coronary Artery (LCFX). Mean CAC in LAD was 89.92±255.60, 80.72±367.64 in RCA and 12.58±58.25 in LCFX, table (4.2). Plaques appear as calcified in 30 out of101patient, mixed in 9, non-calcified in 11, soft in1, and no presence of plaque in 50 patients. In all arteries the plaques took place at different locations; proximal, middle, distal, both proximal & middle, proximal & distal, middle & distal segments, these were presented in tables (4.3and 4.4)

The cases were diagnosed by expert radiologist, the findings were that there were different degrees of atherosclerotic changes including mild, moderate and severe, total occlusion, severe stenosis and severe calcifications and pericarditis were also found.

In the diagnosis of atherosclerotic vessels; the mean calcium values presented in the coronary arteries were found to be 0-346.0, 0-162.0, and 0-9 Agatston in LAD, RCA and LCFX in respectively table (5). It is known that CAC is path gnomonic for atherosclerosis [Blankenhorn DH et.al 1959; Frink RJ et al, 1970; Wexler L et al, 1996] Atherosclerosis is the only vascular disease known to be associated with coronary calcification, these were the findings of our study; the relation is found to be significant between the calcium scoring and the degree of atherosclerotic changes found in all of the investigated coronary arteries.

The presence of CAC is nearly 100% specific for atherosclerosis[Matthew Jet al ,2010], However individuals with zero CAC scores have not yet developed detectable calcified coronary plaque but they may have fatty streaking and early stages of plaque ,therefore it should be taken seriously as the presence of symptoms. In the definitive study [Detrano R et al, 2008], 0 CAC was associated with a 0.11% annual event rate. In another study [Blaha M et al, 2009], the coronary event rate was 0.13% per year in the 25,903 patients with 0 CAC compared to 1% per year for the 42,283 with CAC > 0. In an analysis of all-cause mortality in 44,052 asymptomatic patients followed for 5.6 years [Blaha M et al, 2009], the deaths/1,000 patient years for the 19,898 with 0 CAC was 0.87, compared to 1.92 for CAC 1–10, and 7.48 for CAC > 10.Therefore critical care should be considered in similar patients findings in order to avoid any unsuspected complications.

The relationship of CAC to obstructive disease has been extensively investigated, [O'Rourke RA et al, 2000] it is not particular for obstructive disease since both obstructive and non-obstructive lesions have calcification present in the intima. Our study showed a significant relation between the calcium scoring values and the presence of stenosis as mild stenosis, severe stenosis, severe calcification, and total occlusion, in LAD the maximum calcium scoring values were found to be 1806.00

in the severe stenosis, and 167.00 in the total occlusion, as well as in RCA; the severe calcification were found to be 2918.0 Agatston where total occlusion cases have only 3.0 Agatston with insignificant relation. In LCFX, the mild and moderate stenosis have higher calcium scoring 268.0 and 5.8.0 Agatston in respectively, where the diagnosed cases as total occlusion have calcium values of 7.0 Agatston this were presented in table (5) .Comparisons of our results with other studies ,the pathology findings have shown that the degree of luminal narrowing is weakly correlated with the amount of calcification [Simons DB et.al 1992; Detrano R et.al 1995; Mautner GC et.al 1994] whereas the likelihood of significant obstruction increases with the total CAC score [Guerci AD et.al 1997].

Presence of Coronary plaque and atherosclerosis is considered as a potentially life-threatening disease [Libby P et.al 1998]. Studies suggest that atherosclerotic plaque pattern is important predictors of plaque stability [Newby AC et.al 1999]. The risk of plaque rupture depends on plaque composition, most ruptures occur in plaques containing a soft, lipid-rich core that is covered by a thin and inflamed cap of fibrous tissue [Virmani R et.al 2000]. Ruptures may be clinically silent, but may cause sudden death [Dalager-Pedersen S et.al 1998] Thus, the detection and classification of coronary lesions would constitute an important forward step in patients with suspected coronary artery disease (CAD). Coronary calcification scores were used as parameters to identify patients at risk of CAD [Raggi P et.al 2000]

MDCT scanners allow for the scanning acquisition with excellent temporal resolution [Klingenbeck RK et.al 1999; Ohnesorge B et.al 2000] as well as the increased scan speed allows for single breath-hold examinations with thinner collimated slice widths. Thus, improved spatial and contrast resolution which was achieved in the CT angiography of the coronary arteries. This does not only allow for the detection of coronary lesions, but also for the differentiation of lesion

configuration. Therefore we use MDCTA for characterization of coronary arteries plaques and correlate the findings with the calcium scoring (Agatston) values. Recently, MDCT has been introduced to detect and classify the non-calcified coronary plaques [Leber AW et al, 2003; Schroeder S et al, 2001]. So far, no data is available on the clinical feasibility of MDCT to determine the composition of coronary plaques. Moreover, the prognostic impact on non-calcified plaques needs to be evaluated and to be compared with coronary calcium scoring. We, therefore, initiated this study in patients with chest pain and suspected to have CAD to evaluate whether plaque characterization have correlation with calcium scoring detected by MDCT scanners.

Table (4.6)shows that the calcium scoring values were found to be 1806.0 , 2918.0 and 508.0 for calcified plaque ,where non calcified plaques were 747.0, 2012.0 and 40.0, mixed plaques constituting 538.0, 25.0 and 11.0, soft plaques were found to be zero ,3.0 and 7.0 Agatston ,and patients who were diagnosed as normal, the calcium score values were730.0, 31.00 and 40.00 Agatston for LAD, RCA and LCFX in respectively with no significant relationship at p value 0.005 between the plaque type and calcium scoring Agatston values. Considering the coronary calcium values it is considered as a marker for total plaque troubles. Studies suggested that future coronary events may be predicted on the basis of the calcium score [Wayhs R et al ,2002; Wong ND et al 2002; Detrano RC et al ,2000; Pohle K et al 2003; O'Malley PG et al 2000]

The importance of calcium measurements reveals the effect of treatment [Callister T et al, 1998; Achenbach S et al, 2002]. However, there are query among the coronary plaques consist of non-calcified tissue [Virmani R et al, 2000; Kragel A et al, 1989]. Thus, even in coronary vessels without calcified plaques, severe atherosclerosis may be present. Furthermore, non-calcified lesions may also

developed for acute coronary events [Leber AW et al, 2003] Hence, a more precise assessment of coronary plaque and characterization of calcified and non-calcified plaques can be expected to add important information. Regarding this statement and our results; if the patient came with symptoms of chest pain and zero calcium score in the coronary arteries it should be taken seriously considering the presence of symptoms and this needs more care and should be advised for further investigations.

The usage of CAC scanning as a risk assessment tool may consider as one of the most important advances in the medical radiological field. It offers identifying the patients intended to have cardiac events, diagnosis of coronary arteries lesions as well as characterizing the plaque types and, in so doing, should allow for reduction of cardiovascular mortality and morbidity by increasingly the diagnostic radiological value and defining the treatment schedule on coronary arterial calcification and to determine whether changes in coronary arterial calcification in individual patients have an indicative value for future coronary events. It is believable that measurements of calcium score by MDCT will provide an acknowledged analytical radiological tool.

5.2. Conclusion

Coronary atherosclerosis resulting in ‘fixed’ obstruction is the major cause of IHD in more than 90% cases. The general aspects of atherosclerosis as regards its etiology, pathogenesis and the morphologic features of atherosclerotic lesions have already been dealt with at length this study. This study was designed to define the role of computed tomography coronary angiography (CTA) in the diagnosis of patients with chest pain and suspected to have coronary artery disease (CAD) by measuring the calcium scoring in the coronary arteries (CAC) and correlate the results with the (CTA) findings and coronary arteries plaque types. A 101 patients (59 male, 42 female; mean age, 58.98 years) underwent (CTA). Quantitative coronary angiography calcium scoring (Agatston) was measured in right coronary artery (RCA), left anterior descending artery (LAD), left circumflex coronary artery (LCFX). The main finding of this study was; Plaque types were calcified in 29.7%, non-calcified in 10.9%, mixed in 8.9% and soft plaque in 1.0%. (CTA) findings were mild, moderate and severe atherosclerosis, coronary arteries stenosis, total occlusion and pericarditis. A significant relationship was noticed between the calcium scoring values and the (CTA) findings in both (LAD) and (RCA) at p value<0.05, with no significant relation between the plaque type and calcium scoring Agatston values in (RCA) and (LCFX) was identified. This was lead to conclude that the CAC scoring having superior role in diagnosing and early management of CAD by estimating and diagnosing of many of its problem using MDCT scan.

Finally (CAC) offers identifying the patients intended to have cardiac events, diagnosis of coronary arteries lesions and characterizing the plaque pattern .It is believable that measurements of calcium score will provide an acknowledged analytical radiological tool for the diagnoses of (CAD).

5.3. Recommendation:

- Finally (CAC) offers identifying the patients intended to have cardiac events, diagnosis of coronary arteries lesions and characterizing the plaque pattern .It is believable that measurements of calcium score will provide an acknowledged analytical radiological tool for the diagnoses of (CAD).
- Increasing knowledge and research in coronary artery angiography and its benefits con be very important to the patient and to the cardiologist in term of management actions
- This study was identified that the CAD can be detected more accurately using ultrafast MDCT by quantifying the amount and type of calcium collection in arterial lumen.
- For future and upcoming research it’s important to increase the number of the patient of more finding.

References

Agatston AS, Janowitz WR, Hildner FJ, et al. Quantification of coronary artery calcium using ultrafast computed tomography. J Am CollCardiol. 1990; 15: 827

American Heart Association. Heart and Stoke Statistical Update. Dallas, TX: American Heart Association; 2001.

Arad Y, Goodman KJ, Roth M, et al. Coronary calcification, coronary risk factors, and atherosclerotic cardiovascular disease events. The St Francis Heart Study. J Am CollCardiol. 2005; 46 (1):158–165.

Baumgart D, Schmermund A, Goerge G, et al. Comparison of electron beam computed tomography with intracoronary ultrasound and coronary angiography for detection of coronary atherosclerosis. J Am CollCardiol. 1997; 30: 57–64.

Becker CR, Kleffel T, Crispin A, et al. Coronary artery calcium measurement. Agreement of multirow detector and electron beam CT. Am J Roentgenol. 2001; 176: 1295–1298.
Blankenhorn DH, Stern D. Calcification of the coronary arteries. Am J Roentgenol. 1959; 81: 772–777.

Blobel J, Baartman H, Rogalla P, Mews J, Lembcke A. Spatial and temporal resolution with 16-slice computed tomography for cardiac imaging. Fortschr Roentgenstr. 2003; 175: 1264–1271.

Bluemke DA, Achenbach S, Budoff M, et al. Noninvasive coronary artery imaging: magnetic resonance angiography and Multidetector computed tomography angiography: a scientific statement from the american heart association committee on cardiovascular imaging and intervention of the council on cardiovascular radiology and intervention, and the councils on clinical cardiology and cardiovascular disease in the young. Circulation. 2008; 118(5):586–606.
Boerma E et al: Acute myocardial infarction. Lancet 361:847, 2003.

Bostrom K, Watson KE, Horn S, et al. Bone morphogenetic protein expression in human atherosclerotic lesions. J Clin Invest. 1993; 91: 1800–1809.

Budoff MJ, Achenbach S, Blumenthal RS, et al. Assessment of coronary artery disease by cardiac computed tomography, a scientific statement from the American Heart Association Committee on Cardiovascular Imaging and Intervention, Council on Cardiovascular Radiology and Intervention, and Committee on Cardiac Imaging, Council on Clinical Cardiology. Circulation. 2006; 114(16):1761–1791.

Budoff MJ, Dowe D, Jollis JG, et al. Diagnostic performance of 64-detector row coronary computed tomographic angiography of individuals undergoing invasive coronary prospective multicenter ACCURACY (Assessment by Coronary Computed Individuals Without Known Coronary Artery Disease: Results From the Tomographic Angiography for Evaluation of Coronary Artery Stenosis in Angiography) trial. J Am CollCardiol. 2008; 52(21):1724–1732.

Budoff MJ, Ehrlich J, Hecht HS, Rumberger JR. Letter to the editor. JAMA. 2004; 291: 1822.

Budoff MJ, Nasir K, McClelland RL, et al. Coronary calcium predicts events better with absolute calcium scores than age-gender-race percentiles– The Multi-Ethnic Study of Atherosclerosis (MESA). J AmCollCardiol. 2009; 53: 345–352.

Budoff MJ. Maximizing dose reductions with cardiac CT. Int J Cardiovasc Imaging. 2008; PMID: 19115082.

Callister TQ, Cooil B, Raya SP, et al. Coronary artery disease: improved reproducibility of calcium scoring with an electron-beam CT volumetricmethod. Radiology. 1998; 208: 807–814.

Carr JJ, Nelson JC, Wong ND, et al. Calcified coronary artery plaque measurement with cardiac CT in population-based studies: standardized protocol of Multi-Ethnic Study of Atherosclerosis (MESA) and Coronary Artery Risk Development in Young Adults (CARDIA) study. Radiology. 2005; 234: 35–43.

Chopra P: Illustrated Textbook of Cardiovascular Pathology. New Delhi, Jaypee Brothers Medical Publisher (P) Ltd., 2003.

Corri R et al: Pathogenetic concepts of acute coronary syndromes. J Am CollCardiol41:7S, 2003.

Daviglus ML, Pirzada A, Liu K, et al. Comparison of low risk and higher risk profiles in middle age to frequency and quantity of coronary artery calcium years later. Am J Cardiol. 2004; 94: 367–369.

De Backer G, Ambrosioni E, Borch-Johnson K, et al. European guidelines on cardiovascular disease prevention in clinical practice. Third joint task force of European and other societies in cardiovascular disease prevention in clinical practice. Eur J CardiovascPrevRehabil. 2003; 10 (suppl 1):S1–S10.

Detrano R, Guerci AD, Carr JJ, et al. Coronary calcium as a predictorof coronary events in four racial or ethnic groups. N Engl J Med. 2008; 358: 1336–1345.

Dewey M, Laule M, Krug L, et al. Multisegment and halfscan reconstruction of 16-slice computed tomography for detection of coronary artery stenosis. Invest Radiol. 2004; 39: 223–229.

Duerinckx AJ, Urman MK, Atkinson DJ, Simonetti OP, Sinha U, Lewis B. Limitations of MR coronary angiography. J MagnReson Imaging. 1994; 4: 81.

Duerinckx AJ, Urman MK. Two dimensional coronary MR angiography: analysis of initial clinical results. Radiology. 1994; 193: 731–738.

Faber A. Die Arteriosklerose, from PathologischeAnatomie, from Pathogenese Und Actiologie. In: G. Fischer, ed; 1912.

Frazer WJ et al: Rheumatic Aschoff nodule revisited. Histopathology 27: 457, 1995.

Frink RJ, Achor RWP, Brown AL, et al. Significance of calcification of the coronary arteries. Am J Cardiol. 1970; 26: 241–247.

Gerber TC, Carr JJ, Arai AE, et al. Ionizing radiation in cardiac imaging: a science advisory from the American Heart Association Committee on Cardiac Imaging of the Council on Clinical Cardiology and Committee on Cardiovascular Imaging and Intervention of the Council on Cardiovascular Radiology and Intervention. Circulation. 2009; 119(7): 1056–1065.

Gopal A, Mao SS, Karlsberg D, et al. Radiation reduction with prospective ECG-triggering acquisition using 64-multidetector computed tomographic angiography. Int J Cardiovasc Imaging. 2009; 25(4):405–416.

Greenland P, LaBree L, Azen SP, et al. Coronary artery calcium score combined with Framingham score for risk prediction in asymptomatic individuals. JAMA. 2004; 291: 210–215.

Guilherme L, Kalil J: Rheumatic fever: from sore throat to autoimmune heart lesions. Int Arch Allergy Immunol134:56, 2004.

Hecht HS, Superko HR, Smith LK, et al. Relation of coronary artery calcium identified by electron beam tomography to serum lipoprotein levels and implications for treatment. Am J Cardiol. 2001; 87:406–412.

Hecht HS, Superko HR. Electron beam tomography and national cholesterol education program guidelines in asymptomatic women. J Am CollCardiol. 2001; 37: 1506–1511.

Hill EE et al: Evolving trends in infective endocarditis. Clin Microbiol Infect 12:5, 2006.

Hirota S, Imakita M, Kohri K, et al. Expression of osteopontin messenger RNA by macrophages in atherosclerotic plaques. A possible association with calcification. Am J Pathol. 1993; 143: 1003–1008.

Hoffmann U, Bamberg F, Chae CU, et al. Coronary computed tomography angiography for early triage of patients with acute chest pain – the Rule Out Myocardial Infarction using Computer Assisted Tomography (ROMICAT) trial. J Am CollCardiol. 2009; 53(18):1642–1650.

Hofman MB, Wickline SA. Quantification of in-plane motion of the coronary arteries during the cardiac cycle: implications for acquisition window duration for MR flow quantification. J MagnReson Imaging. 1998; 8(3):568–576.

Hunold P, Vogt FM, Schmermund A, et al. Radiation exposure during cardiac CT: effective doses at multi-detector row CT and electronbeamCT. Radiology. 2003; 226: 145–152.

ICRP (ICoRP). The 2007 recommendations of the International Commission on Radiological Protection (ICRP Publication 103). Ann ICRP. 2007; 37: 1–332.

Ideda T, Shirasawa T, Esaki Y, et al. Osteopontin mRNA is expressed by smooth muscle-derived foam cells in human atherosclerotic lesions of the aorta. J Clin Invest. 1993; 92: 2814–2820.

Jakobs TF, Becker CR, Ohnesorge B, et al. Multislice helical CT of the heart with retrospective ECG gating: reduction of radiation exposure by ECG-controlled tube current modulation. EurRadiol. 2002; 12: 1081–1086.

Kim WY, Danias PG, Stuber M, et al. Coronary magnetic resonance angiography for the detection of coronary stenoses. N Engl J Med. 2001; 345: 1863–1869.

Kuller LH, Matthews KA, Sutton-Tyrrell K, et al. Coronary and aortic calcification among women 8 years after menopause and their premenopausal risk factors: The Healthy Women Study. Arterioscler ThrombVasc Biol. 1999; 19: 2189–2198.

Leber AW, Knez A, von Ziegler F, et al. Quantification of obstructive and nonobstructive coronary lesions by 64-slice computed tomography: a comparative study with quantitative coronary angiography and intravascular ultrasound. J Am CollCardiol. 2005; 46: 147–154.

Leber AW, Knez A, White CW, et al. Composition of coronary atherosclerotic plaques in patients with acute myocardial infarction and stable angina pectoris determined by contrast-enhanced multislice computed tomography. Am J Cardiol. 2003; 91: 714–718.

Lembcke A, Rogalla P, Mews J, et al. Imaging of the coronary arteries by means of multislice helical CT: optimization of image quality with multi-segmental reconstruction and variable gantry rotation time. Fortschr Roentgenstr. 2003; 175: 780–785.

Lessick J, Dragu R, Mutlak D, et al. Is functional improvement after myocardial infarction predicted with myocardial enhancement patternsat multidetector CT? Radiology. 2007; 244: 736–744.

Lipton MJ, Higgins CB, Boyd DP. Computed tomography of the heart: evaluation of anatomy and function. J Am CollCardiol. 1985; 5: 555–595.

Manning WJ, Li W, Edelman RR. A preliminary report comparing magnetic resonance imaging with conventional angiography. N EnglJ Med. 1993; 328: 828–832.

Mao S, Lu B, Oudiz RJ, BakhsheshiH, Liu SCK, Budoff MJ. Coronary artery motion in electron beam tomography. J Comput Assist Tomogr.2000;24:253–258.

Mao SS, Budoff MJ, Oudiz RJ, et al. Effect of exercise on left and right ventricular ejection fraction and wall motion in patients with coronary artery disease: an electron beam computed Tomography study. Int J Cardiol. 1999; 71: 23–31.

Marcus JT, Smeenk HG. Flow profiles in the left anterior descending and the right coronary artery assessed by MR velocity quantification: effects of through-plane and in-plane motion of the heart. J Comput Assist Tomogr. 1999; 23(4):567–576.

Maron BJ et al: AHA scientific statement. Contemporary definitions and classification of cardiomyopathies. Circulation 113:1087, 2006.

Mascola A, Ko J, Bakhsheshi H, et al. Electron beam tomography comparison of culprit and non-culprit coronary arteries in patients with acute myocardial infarction. Am J Cardiol. 2000; 85: 1357–1359.

McKay CR, Brundage BH, Ullyot DJ, et al. Evaluation of early postoperative coronary artery bypass grafts patency by contrastenhancedcomputed tomography. J Am CollCardiol. 1983; 2: 312–317.

Mintz GS, Painter JA, Pichard AD, et al. Atherosclerosis in angiographicallynormal coronary artery reference segments: an intravascular ultrasound study with clinical correlations. J Am CollCardiol. 1995; 25: 1479–1485.

Morin RL, Gerber TC, McCollough CH. Radiation dose in computed tomography of the heart. Circulation. 2003; 107: 917–922.

Mosca L, Appel LJ, Benjamin EJ, et al.; Expert Panel/Writing Group. Evidence-based guidelines for cardiovascular disease prevention in women. Circulation. 2004; 109: 672–693.

Mylonkis E, Calderwood SB: Infecive endocarditis in adults. N Engl J Med 345: 1318, 2001.

Naghavi M, Falk E, Hecht HS, et al. From vulnerable plaque to vulnerable patient – part III: executive summary of the Screening for Heart Attack Prevention and Education (SHAPE) Task Force Report. Am J Cardiol. 2006; 98 (suppl):2H–15H.

Napel S, Rubin GD, Jeffrey RB Jr. STS-MIP: A new reconstruction technique for CT of the chest. J Comput Assist Tomogr. 1993; 17(5): 832–838.

Nieman K, Rensing BJ, van Geuns RJ, et al. Non-invasive coronary angiography with multislice spiral computed tomography: impact of heart rate. Heart. 2002; 88(5):470–474.

Nissen SE, Gurley GL. Assessment of coronary angioplasty results by intravascular ultrasound. In: Serruys PW, Straus BH, King SB III, eds. Restenosis after Intervention with New Mechanical Devices. Dordrecht, Netherlands: Kluwer; 1992:73–96.

O'Malley PG, Feuerstein IM, Taylor AJ. Impact of electron beam tomography, with or without case management, on motivation, behavioral change, and cardiovascular risk profile: a randomized controlled trial. JAMA. 2003; 289: 2215–2223.

Orakzai RH, Nasir K, Orakzai SH, et al. Effect of patient visualization of coronary calcium by electron beam computed tomography on changes in beneficial lifestyle behaviors. Am J Cardiol. 2008; 101: 999–1002.

Orakzai SH, Orakzai RH, Nasir K, Budoff MJ. Assessment of cardiac function using multidetector row computed tomography. J ComputAssist Tomogr. 2006; 30 (4):555–563.

Paschal CB, Haache EM, Adler LP. Coronary arteries: three-dimensional MR imaging of the coronary arteries: preliminary clinical experience. J MagnReson Imaging. 1993; 3: 491–501.

Pennell DJ, Keegan J, FirminDN, Gatehouse PD, Underwood SR, Longmore DB. Magnetic resonance imaging of coronary arteries: technique and preliminary results. Br Heart J. 1993; 70: 315–326.

Pohle K, Ropers D, Mäffert R, et al. Coronary calcifications in young patients with first, unheralded myocardial infarction: a risk factor matched analysis by electron beam tomography. Heart. 2003; 89: 625–628.

Raggi P, Callister TQ, Cooil B, et al. Identification of patients at increased risk of first unheralded acute myocardial infarction by electron beam computed tomography. Circulation. 2000; 101: 850–855.

Regenfus M, Ropers D, Achenbach S, et al. Noninvasive detection of coronary artery stenosis using contrast-enhanced three-dimensional breath-hold magnetic resonance coronary angiography. J Am CollCardiol. 2000; 36: 44–50.

Ritchie CJ, Godwin JD. Minimum scan speeds for suppression of motion artifacts in CT. Radiology. 1992; 185: 37–42.

Rumberger JA, Simons DB, Fitzpatrick LA, et al. Coronary artery calcium areas by electron beam computed tomography and coronary atherosclerotic plaque area: a histopathologic correlative study. Circulation. 1995; 92: 2157–2162.

Schmermund A, Baumgart D, Gorge G, et al. Coronary artery calcium in acute coronary syndromes: a comparative study of electron beam CT, coronary angiography, and intracoronary ultrasound in survivors of acute myocardial infarction and unstable angina. Circulation. 1997; 96: 1461–1469.

Schroeder S, Kopp AF, Baumbach A, et al. Noninvasive detection and evaluation of atherosclerotic coronary plaques with multislice computed tomography. J Am CollCardiol. 2001; 37: 1430–1435.

Schwartz SM et al: The intima: soil for atherosclerosis and restenosis. Circ Res 77: 445, 1995.
Sethi KK, Verma P: Chlamydial pneumonia and coronary heart disease (Editorial). Cardiol Today 2: 9, 1999.

Shanahan CM, Cary NR, Metcalfe JC, Weissberg PL. High expression of genes for calcification-regulating proteins in human atherosclerotic plaque. J Clin Invest. 1994; 93: 2393–2402.

Silver MD: Cardiovascular Pathology, 2nd ed. London, Churchill Livingstone, 1991.

Stuber M, Botnar RM, Fischer SE, et al. Preliminary report of in-vivo coronary MRA at 3 Tesla in humans. MagnReson Med. 2002; 48: 425–428.

Taylor AJ, Feuerstein I, Wong H, et al. Do conventional risk factors predict subclinical coronary artery disease? Results from the Prospective Army Coronary Calcium Project. Am Heart J. 2001; 141:463–468.

Tegos TJ et al: The genesis of atherosclerosis and risk factors: a review. Angiology 52: 89, 2001.

Trabold T, Buchgeister M, Kuttner A, et al. Estimation of radiation exposure in 16-detector row computed tomography of the heart with retrospective ECG-gating. Rofo. 2003; 175: 1051–1055.

Van den Broek JGM, Slump CH, Storm CJ, Van Benthem AC, Buis B. Three-dimensional densitometric reconstruction and visualization of stenosed coronary artery segments. Comput Med Imaging Graph. 1995; 19: 207–217.

Wang Y, Vidan E. Cardiac motion of coronary arteries: variability in the rest period and implications for coronary MR angiography. Radiology. 1999; 213 (3):751–758.

Wexler L, Brundage B, Crouse J, et al. Coronary artery calcification: pathophysiology, epidemiology, image methods and clinical implications. A scientific statement from the American Heart Association. Circulation. 1996; 94: 1175–1192.

Wicky S, Rosol M, Hoffmann U, Graziano M, Yucel KE, Brady TJ. Comparative study with a moving heart phantom of the impact of temporal resolution on image quality with two multidetector electrocardiography-gated computed tomography units. J Comput AssistTomogr. 2003; 27: 392–398.

Wu YW, Tadamura E, Yamamuro M, et al. Estimation of global and regional cardiac function using 64-slice computed tomography: a comparison study with echocardiography, gated-SPECT and cardiovascularmagnetic resonance. Int J Cardiol. 2008; 128: 69–76.

Appendix

Example of master data sheet was used in data collection

age	gender	heart rate	LAD	RCA	LXR	Affected artery
63	1	52	346	162	7	RCA
60	2	61	0	3	0	RCA
58	1	65	0	0	0	NORMAL
72	1	62	73	0	40	LAD+LCX
58	1	65	0	0	0	NORMAL
65	1	68	2	0	0	RCA
62	1	61	0	0	0	NORMAL
59	1	65	0	0	0	NORMAL
75	2	66	0	0	0	NORMAL
30	2	60	0	0	0	NORMAL
55	1	68	0	0	0	NORMAL
75	1	66	1	21	0	RCA
66	1	62	0	2	0	NORMAL
54	2	59	0	0	0	NORMAL
80	1	66	0	24	0	RCA
70	2	65	31	0	31	RCA+LAD
46	2	66	0	0	0	NORMAL
59	1	61	88	2	0	RCA+LAD
64	2	59	0	0	0	NORMAL
55	1	66	10	0	0	NORMAL
49	2	63	0	0	0	NORMAL
45	2	57	67	0	11	NORMAL
46	1	59	0	0	0	NORMAL
76	2	65	0	0	0	NORMAL
70	2	66	81	5	0	LAD
49	1	63	0	0	0	NORMAL
69	1	69	23	1	0	RCA+LAD
57	1	59	56	2012	5	RCA+LAD+LCX
42	1	52	0	0	0	NORMAL
87	1	55	0	22	1	RCA+LAD
58	1	67	0	0	0	NORMAL
58	1	65	0	0	0	NORMAL
60	1	59	0	0	0	LAD+LCX
65	1	66	9	25	11	RCA+LAD

60	1	55	0	0	0	NORMAL
60	1	60	0	31	0	RCA
54	2	69	51	31	0	RCA+LAD
45	2	69	51	31	0	NORMAL
49	1	55	0	0	0	NORMAL
66	1	64	0	0	0	NORMAL
70	1	63	0	0	0	RCA
41	2	61	0	31	9	RCA+LXR
65	1	66	90	513	0	RCA+LAD
61	1	55	21	19	237	RCA+LAD+LXR
69	2	66	0	0	0	NORMAL
55	1	61	0	21	0	RCA
66	2	65	22	300	0	RCA+LAD
53	1	55	0	0	0	NORMAL
59	2	66	30	2	7	RCA+LAD+LXR
60	2	63	0	0	0	NORMAL
59	1	66	2	0	1	RCA+LXR
10	1	60	0	0	0	NORMAL
60	1	66	0	0	0	RCA+LAD+LXR
50	1	55	18	0	0	LAD
44	1	66	0	0	0	NORMAL
61	2	63	5	0	1	LAD+LXR
60	2	59	6	0	0	LAD
69	1	65	35	0	0	LAD
54	2	60	0	3	0	RCA
59	1	66	0	0	0	NORMAL
63	2	61	0	0	0	LAD, D1
66	1	59	0	0	0	LCX
49	2	63	0	31	2	LAD
50	1	66	17	2	1	LAD
70	2	65	31	0	2	RCA+LAD
59	1	60	81	2	0	LAD
72	1	62	730	1	40	LAD+LCXR
60	2	59	1	40	9	LAD+RCA
50	2	69	0	0	0	NORMAL
49	1	65	538	20	1	LAD+RCA
59	2	55	1011	50	11	LAD+RCA
67	2	63	0	0	0	NORMAL
69	2	61	22	1011	30	RCA+LAD+LXR
49	1	66	13	0	0	LAD
55	1	63	0	0	0	NORMAL

53	2	66	747	300	40	RCA+LAD+LXR
64	2	59	0	0	0	LAD+RCA
55	1	69	10	1	0	NORMAL
58	1	65	167	0	0	LAD
45	2	63	67	0	11	LAD
62	1	65	0	0	0	NORMAL
68	1	65	4	0	0	LAD
60	1	62	0	0	0	RCA
70	2	66	0	0	0	LCX
75	1	65	1806	235	508	RCA+LAD+LXR
50	2	66	0	0	0	NORMAL
60	2	68	0	0	0	NORMAL
70	1	61	510	21	53	LAD
70	1	65	511	0	0	LAD
65	2	69	538	227	10	RCA+LAD+LXR
56	1	66	0	3	7	LAD+RCA
59	2	63	53	0	7	LAD
35	1	67	0	0	0	NORMAL
48	2	66	0	0	0	NORMAL
61	1	58	327	2918	3	RCA+LAD+LXR
60	2	66	0	0	0	NORMAL
50	1	63	0	0	0	NORMAL
60	2	65	0	9	0	RCA
80	1	62	33	11	0	RCA
55	2	64	0	0	0	NORMAL
65	2	69	747	10	175	RCA+LAD+LXR

Continue

D. of stenosis	plaque type	location of lesion	Result
2	1	NORMAL	SEVER RCA LESION
1	1	mid+dis segement	RCA LESION
0	0	NORMAL	NORMAL
1	0	dis+pro	PERCARDITIS
0	0	NORMAL	NORMAL
2	0	pro	SEVER RCA LESION
0	0	NORMAL	NORMAL
0	0	NORMAL	NORMAL
0	0	NORMAL	NORMAL
0	0	NORMAL	NORMAL

0	0	NORMAL	NORMAL
1	0	pro	MILD RCA LESION
0	0	NORMAL	NORMAL
0	0	NORMAL	NORMAL
0	3	mid	NORMAL
2	1	mid	MILD STENOSIS
0	0	NORMAL	NORMAL
1	1	pro LAD	SEVER LAD STENOSIS
0	0	NORMAL	NORMAL
0	0	NORMAL	NORMAL
0	0	NORMAL	NORMAL
0	0	NORMAL	NORMAL
0	0	NORMAL	NORMAL
0	0	NORMAL	NORMAL
2	1	MID	MILD LAD STENOSIS
0	0	NORMAL	NORMAL
2	2	PRO +MID	RCA LESION
3	2	PRO RCA+MID LAD	
0	0	NORMAL	NORMAL
1	3	MID	MILD LAD LESION
0	0	NORMAL	NORMAL
0	0	NORMAL	MILD RCA+LAD LESION
1	2	MID RCA+LAD	MILD RCA+LAD LESION
1	3	PRO LAD	NORMAL
0	0	NORMAL	RCA LESION
1	1	MID	MILD RCA LESION
1	1	MID RCA	MILD RCA LESION
0	0	NORMAL	NORMAL
0	0	NORMAL	NORMAL
0	0	NORMAL	NORMAL
1	2	NORMAL	MILD STENOSIS
1	1	MID	LXR+RCA LESION
3	1	MID RCA+LAD	SVER RCA STENOSIS
1	1	MID RCA	STENOSIS
0	0	NORMAL	NORMAL
1	2	DIS	MILD RCA STENOSIS
MILD LAD, SEVER RCA	1	MID RCA+DIS LAD	RCA+LAD STENOSIS

0	0	NORMAL	NORMAL
1	1	MID	NORMAL
0	0	NORMAL	NORMAL
0	2	DIS	NORMAL
0	0	NORMAL	NORMAL
1	2	MID	MILD STENOSIS
0	1	NORMAL	NORMAL
0	0	NORMAL	NORMAL
MILD LAD	2	NORMAL	NORMAL
1	0	NORMAL	NORMAL
0	1	MID	NORMAL
1	3	MID RCA	RCA+LAD STENOSIS
0	0	NORMAL	NORMAL
0	2	DIS D1	NORMAL
0	3	MID	MILD STENOSIS
0	0	NORMAL	
0	0	NORMAL	NORMAL
2	1	MID	MILD STENOSIS
1	1	PRO	SEVER LAD STENOSIS
1	0	DIS LAD+PRO LXR	PERCARDITIS
1	2	MID	MILD STENOSIS
0	0	NORMAL	NORMAL
1	3	DIS RCA+LAD	LAD STENOSIS
SEVER, LAD, MILD, RCA	1	PRO LAD	SEVER CALCIFICATION
0	0	NORMAL	NORMAL
3	1	MID RCA+DIS LAD	SEVER RCA, MILD LAD
1	1	MID LAD	D1 LAD STENOSIS
0	0	NORMAL	NORMAL
3	2	PRO RCA+MID LAD	SEVER RCA STENOSIS
2	1	MID RCA	MODERATE LAD, MILD RCA
0	0	NORMAL	NORMAL
1	1	PRO+DIS	CALCIFIED LAD
2	1	PRO LCX+LAD	LCX STENOSIS
0	0	NORMAL	NORMAL
0	1	PRO	NORMAL
2	3	PRO	MODERATE RCA
1	1	PRO	NORMAL

MODERATE LAD, MILDLCX	1	PRO RCA+LAD+LXR	SEVER STENOSIS
0	0	NORMAL	NORMAL
0	0	NORMAL	NORMAL
0	1	PRO	MILD LXC STENOSIS
0	3	DIS	LAD STENOSIS
3	1	PRO RCA+LAD+LXR	SVER STENOSIS
3	3	MID LAD	TOTAL OCCULION
1	3	PRO	MILD LAD STENOSIS
0	0	NORMAL	NORMAL
0	0	NORMAL	NORMAL
3	1	PRO RCA+MID LAD	SEVER CALCIFICATION
0	0	NORMAL	NORMAL
0	0	NORMAL	NORMAL
0	0	NORMAL	RCA LESION
2	1	PRO+MID	RCA STENOSIS
0	0	NORMAL	NORMAL
3	1	PRO RCA+LAD+LXR	SEVER STENOSIS